A historical perspective on the regulation of cellulose biosynthesis

Holly Allen[a], Donghui Wei[a], Ying Gu[a] and Shundai Li[ab]

[a]Department of Biochemistry and Molecular Biology, The Pennsylvania State University, University Park, PA, 16802, USA (hea5112@psu.edu, dxw608@psu.edu, yug13@psu.edu)

[b]Address correspondence to sul38@psu.edu

Highlights

- Many aspects of cellulose synthesis are shared between bacteria, algae, and higher plants.
- Significant progress has been made in studying the physical aspects of cellulose synthesis due to the development of more sensitive techniques.
- Cellulose microfibrils are important for anisotropic cell expansion.
- Live-cell imaging has greatly enhanced the study of cellulose synthesis.

Abstract

Cellulose is a β-1,4 linked glucose polymer that is synthesized by higher plants, algae and even by some bacteria and animals, making it the most abundant polymer on earth. As the major load bearing structure of the plant cell wall, it is hugely important in terms of plant growth and development, and in recent years it has gained interest for its biotechnological applications. Naturally, there has been a large, concerted research effort to uncover the regulatory mechanisms underpinning cellulose synthesis. During the last century, several major breakthroughs in our understanding of cellulose synthesis in unicellular organisms and higher plants have been pivotal in advancing the field of cellulose research, improving the likelihood that cellulose synthesis could be feasibly adapted for sustainable purposes. In this review, we will summarize the major hypotheses and advancements made during the last century on the regulation of cellulose biosynthesis, focussing on *Arabidopsis thaliana.*

Keywords: cell wall, synthase complexes, microtubules, trafficking, *Arabidopsis thaliana*

1. Introduction

For centuries, cellulose has been widely recognized in terms of its economic potential and biological influence. Cellulose is an essential multi-purpose resource that is heavily used in construction, paper manufacturing, textile production, and as a source of fuel. More recently, cellulose has been recognized as a potential feedstock for renewable biofuels and other sustainable products. All plant cells deposit cell walls that contain cellulose. As a result, cellulose is the most abundant organic polymer on earth, contributing between 150-170 billion tons of carbon to the biosphere per year through carbon sequestration (Engelhardt, 1995). During growth, plant cells develop a primary cell wall that consists of three main polymers: cellulose, hemicellulose (typically xyloglucan), and pectin, contained within an aqueous matrix (Cosgrove & Jarvis, 2012). Once cells cease expanding, specialized cell types can deposit a thicker, stronger secondary cell wall that is reinforced by the hydrophobic polymer lignin. Cellulose tends to be more abundant in secondary cell walls that are comprised of up to 50% cellulose (Meents, Watanabe, & Samuels, 2018).

Despite its huge importance, cellulose research consisted of a relatively finite, insignificant field a hundred years ago. Since the 1950s, several major breakthroughs in our understanding of cellulose synthesis and regulation have turned this on its head and it is now a thriving field of research. Studies historically focussed on characterizing the structure of cellulose microfibrils and synthetic mechanisms in cellulose-rich unicellular organisms, including the green algae, *Valonia* and *Oocystis* and the bacteria *Acetobacter xylinum*. In addition, fibers from *Gossypium* (Cotton) and *Boehmeria* (Ramie) were also used. Ground-breaking findings from these organisms were applied to higher plants on the basis that the intrinsic properties of cellulose were shared, igniting the study of cellulose synthesis in higher plants. The development of the herbaceous species, *Arabidopsis thaliana,* as a model plant for genetic research in the 1980s caused a noticeable shift from studying the biophysical aspects of cellulose to a genetic and cell biology led approach, especially regarding the dynamics of the cellulose synthase complex (CSC). In *Arabidopsis*, significant advancements have been somewhat restricted to the primary cell wall, since *Arabidopsis* undergoes limited secondary growth, though some notable contributions have been made (Strabala & Macmillan, 2013). Poplar became a genetic model for studying cellulose in secondary cell walls and is frequently used to validate assumptions made from *Arabidopsis,* and other species, regarding secondary cell wall formation. Poplar can also produce a gelatinous, 'G-layer' that is composed almost entirely of cellulose during tension wood formation, which has greatly supplemented studies of cellulose synthesis (Felten & Sundberg, 2013).

The increasing availability of biological tools combined with the development of highly sensitive techniques have been largely responsible for the significant progress made in the study of cellulose synthesis in higher plants. Together these have confirmed many of the original hypotheses made and answered, at least partially, many of the outstanding questions regarding cellulose synthesis. In this review, we will focus on how our understanding of the regulation of cellulose synthesis has developed during the last century, with particular focus on i) how cellulose is synthesized?; ii) when it is synthesized?; iii) CSC trafficking; and iv) how it is regulated? We will cover the main hypotheses regarding cellulose synthesis, and the significant advancements that have been made to support these in *Arabidopsis,* though contributions from other species will be included where relevant. We regret that due to space limitations we cannot cover every aspect of cellulose synthesis, but some excellent reviews are widely available (Brown & Saxena, 2000; Delmer, 1999; Guerriero, Fugelstad, & Bulone, 2010; Haigler & Roberts, 2018; Lampugnani et al., 2019; Li, Bashline, Lei, & Gu, 2014; Somerville, 2006; Wolf, Hematy, & Hofte, 2012).

2. How is cellulose synthesized?

The long-standing use of cellulose as a feedstock for the pulping and energy industries naturally called for a more thorough understanding of the physical structure, biochemistry, and synthesis of microfibrils. Early studies on the physical aspects of cell walls and cellulose crystallinity relied on a combination of polarizing microscopy, transmission electron microscopy (TEM) and X-ray diffraction analysis of algae and bacteria. Even with the limited resources available, many of these assumptions were held to be true in higher plants when they were later reinforced by genetics.

2.1 Structure of cellulose

While cellulose was first described as a polymer in the 1920s, the crystal structure of cellulose was not resolved until fifty years later. X-ray diffraction analysis of cellulose from ramie fibers and the algae, *Valonia ventricosa*, revealed that cellulose is a crystalline β-1,4 linked glucose polymer (Gardner & Blackwell, 1974). More specifically, cellulose is a two-fold helical structure of alternating cellobiose units, as β-1,4 glycosidic linkages require a 180° rotation of consecutive molecules (Hermans, de Booys, & Maan, 1943). The 120° rotation of β-1,4 bonds is thought to facilitate the inversion of glucose molecules during synthesis (Delmer, 1999). Multiple isoforms of cellulose exist (I-IV), although the most labile form, cellulose I, is produced almost exclusively in nature (Delmer, 1999). Physical and chemical deformations of cellulose I can produce cellulose II-IV isoforms that are inherently more stable.

The idea of the microfibril was first coined by Preston, Nicolai, and Millard (1948) who observed in electron micrographs and X-ray diffraction analyses of *V. ventricosa* that cellulose consists of multiple glucan chains bound together. Characterizing the structure of cellulose I was initially problematic and diverse X-ray diffraction patterns of cellulose I were reported amongst research groups (Preston, 1974). Assessing the structure more intricately with solid-state nuclear magnetic resonance (ssNMR) revealed that cellulose I exists as two distinct forms, Iα and Iβ (Atalla & Vanderhart, 1984). Cellulose Iα exhibits a triclinic structure composed of one chain and cellulose Iβ contains two parallel chains within a monoclinic structure. Cellulose Iα microfibrils predominate in algae and bacteria, whereas in higher plants and tunicates, cellulose Iβ tends to be more abundant, though microfibrils are often comprised of both forms. Within the microfibril, parallel glucan chains are stabilized by intra- and inter-molecular hydrogen bonds. Hydrophobic van der Waals forces can also form between glucan sheets, particularly in aqueous environments (Cousins & Brown, 1997) and so are perhaps more relevant in primary cell walls that have a high water content. In secondary cell walls, cellulose is held together by a higher degree of intra-molecular hydrogen bonding, creating a rigid, crystalline polymer that invokes strong structural support to the cell. In tension wood, cellulose is almost purely crystalline, which is likely related to the production of wood under high tensile stress (Foston et al., 2011).

The properties of cellulose can be measured in terms of its crystallinity; width; degree of polymerization; and cross-sectional shape, to name a few variables. Unsurprisingly, considerable variation in cellulosic properties exists between species, cell types, and even within the microfibril itself. Variations in the width of cellulose microfibrils have been interpreted as differences in the number of glucan chains, the extent of bundling and interactions with non-cellulosic polysaccharides. Measuring microfibrils with a diversity of techniques, including atomic force microscopy (AFM), small-angle neutron scattering (SANS) and wide-angle X-ray scattering (WAXS), have demonstrated that individual microfibrils are consistently 3 – 4 nm wide, across different species and cell wall types (Fernandes et al., 2011; Song, Zhao, Shen, Collings, & Ding, 2020; Zhang, Zheng, & Cosgrove, 2016a). Close microfibril spacing can cause neighbouring microfibrils to associate into larger bundles, that span up to 50 nm in width in secondary cell walls (Anderson, Carroll,

Akhmetova, & Somerville, 2010; Fernandes et al., 2011; Song et al., 2020; Thomas et al., 2013; Zhang et al., 2016a). Detailed examination of microfibrils with AFM has revealed the sheer extent of bundling, particularly in onion primary cell wells where up to ⅔ of the microfibril length coalesces with other microfibrils (Zhang et al., 2016a). Wide cellulose microfibrils also tend to accompany a higher degree of polymerization (DP). In primary cell walls, cellulose DP can range from 500-8,000 and in cotton secondary cell walls, cellulose DP can exceed 15,000 (Brett, 2000). Far longer microfibrils of up to 23,000 DP have been observed in algae that secrete cellulose outside of the cell (Brown, 1996), indicating that microfibril elongation may be partially restricted by the biophysical and spatial constraints of the cell wall. An important caveat is that these estimates of cellulose DP have not yet been verified in the intact cell wall, and so may not be representative of true microfibril DPs. The biological significance of DP and what triggers the termination of chain elongation is unknown, but chain length is likely to be an important determinant of cell wall function and architecture (Somerville, 2006).

Uncovering the structure of cellulose microfibrils formed the building block for all future studies on cellulose, as it can be used as a tool to make logical inferences about the underlying synthetic mechanisms and architecture of cell walls. In particular, the width and cross-sectional shape of cellulose microfibrils has been used to predict the size and arrangement of synthetic complexes and the orientation of microfibrils has informed models of cell expansion. While it has been firmly established that these features of cellulose are highly influential, how many of these cellulosic properties are determined remains an open question.

2.2 Cellulose synthase complexes (CSCs) - Structure

Once the structure of cellulose microfibrils was largely characterized, the next main focus was to identify the protein complex responsible for cellulose synthesis. Uncovering the structure of the synthetic complex was a major breakthrough in cellulose research (Table 1). Twenty years after Roelofsen (1958) correctly predicted that microfibrils extend from the growing tip by large enzyme complexes, linear structures matching that description were identified in the plasma membrane of the algae, *Oocystis apiculate,* by freeze-fracture TEM (Brown & Montezinos, 1976). As they were situated at the base of microfibril imprints they were referred to as ‘terminal complexes’. This was arguably the first indication that cellulose synthesis was highly distinct from other polysaccharides that are synthesized in the Golgi, emphasizing that the production of cellulose in such close proximity to the cell wall has functional significance.

Terminal complexes were subsequently identified in a whole host of different species, including bacteria, higher plants and tunicates (Kimura & Itoh, 1996). However, they were not uniform in their shape, abundance, or organization (Tsekos, 1999). Octagonal arrays and linear rows of rosette complexes in the secondary cell walls of *Micrasteria denticulata* and *Spirogyra* respectively, produce microfibril bundles consisting of more glucan chains than a single rosette in primary cell walls (Giddings, Brower, & Staehelin, 1980; Herth, 1983). In contrast to the linear complexes described in *O. apiculate,* freeze-fractured membranes of maize and pine seedlings revealed that terminal complexes in higher plants consist of rosette-shaped particles with six-fold symmetry (Haigler & Brown, 1986; Mueller & Brown, 1980). Re-examination of rosettes in the moss, *Physcomitrella patens*, has suggested that rosette lobes can be triangular and the six-fold symmetry can be lost due to unequal spacing between lobes (Nixon et al., 2016). In tobacco BY-2 cells the transmembrane region spans 25 nm, similar to predictions made by Mueller and Brown (1980), and the cytosolic region is twice as wide, ranging between 45 - 50 nm (Bowling & Brown, 2008).

Many researchers have repeatedly suggested that differences in the morphology of terminal complexes may be responsible for the diversity in microfibril architecture. In particular, the arrangement of terminal complexes has been linked with the extent of crystallization and microfibril bundling in different types of cell wall (Tsekos, 1999) (Table 1). The closer arrangement of multiple terminal complexes in secondary cell walls may be necessary to facilitate a higher degree of inter-molecular hydrogen bonding between chains. Indeed, in *Arabidopsis*, dispersed complexes produce widely spaced cellulose microfibrils in primary cell walls, whereas in secondary cell walls, dense regions of complexes synthesize highly aggregated crystalline microfibrils (Li et al., 2016). Interestingly, *in vitro* studies of cellulose synthesis have suggested that adjacent microfibrils can spontaneously coalesce to form thicker microfibril bundles in the absence of a rosette complex. Although this indicates that microfibrils may self-assemble in the cell wall, whether these microfibrils resemble *in vivo* structures was not quantified (Cho et al., 2017; Purushotham et al., 2016) and so more rigorous assessment is required to draw this conclusion with great certainty.

The location of terminal complexes at the ends of microfibrils and the high density of rosettes in areas undergoing secondary cell wall deposition (Herth, 1985) made terminal complexes primary candidates for cellulose biosynthesis, however, this evidence was purely circumstantial. Fifteen years after terminal complexes were first visualized in green algae, genes with cellulose synthetic ability were cloned from the bacteria, *A. xylinum* (Saxena, Lin, & Brown, 1990; Wong et al., 1990). The bacterial operon encodes four bacterial cellulose synthase (*Bcs*) genes, *BcsA/B/C/D*, that are members of the glycosyltransferase 2 (GT2) family. Homologs in higher plants were found by screening a cotton cDNA library for sequence similarities with *A. xylinum* (Pear, Kawagoe, Schreckengost, Delmer, & Stalker, 1996). Although the genes from cotton exhibited low sequence homology with *A. xylinum*, as these proteins could bind to UDP-glucose *in vitro* they were putatively named cellulose synthase (CESA) genes. Immuno-labelling of freeze-fractured terminal complexes in azuki beans with CESA-specific antibodies, made the vital connection between cellulose synthesis and terminal complexes and identified CESAs as a component of the terminal complexes (Kimura et al., 1999) (Table 1). As a result, terminal complexes are commonly referred to as cellulose synthase complexes (CSCs).

The exact number of CESA proteins that occur in CSCs has been widely debated and is still an outstanding question in the field (Table 1). Originally, it was speculated that each rosette subunit contains a hexamer of CESA proteins that each synthesize a single chain, producing a 36-chain microfibril (Herth, 1983). Each CESA protein is still proposed to synthesize a single glucan chain, based on strong homology between the catalytic domain of cotton *CESA* proteins and the *Bcs* complex of *Rhodobacter sphaeroides,* that produces a single chain (Morgan, Strumillo, & Zimmer, 2013; Sethaphong et al., 2013). Recent evidence corroborates this hypothesis, as single CESA isoforms purified from rice and poplar are capable of synthesizing cellulose *in vitro* (Olek et al., 2014; Purushotham et al., 2016). However, the 36-chain model has been widely rejected as 3 nm wide microfibrils are simply too narrow to accommodate 36 chains (Fernandes et al., 2011; Newman, Hill, & Harris, 2013; Thomas et al., 2013), and 45 - 50 nm wide cytoplasmic domains of CSCs are predicted to contain a maximum of four CESA proteins per rosette subunit (Bowling & Brown, 2008).

200 **Table 1 -** A summary of the major hypotheses made regarding the regulation of cellulose synthesis.

Original hypothesis	Studies	Current status	Studies
1. Cellulose is synthesized by a terminal complex in the plasma membrane	Observational (Roelofsen, 1958)	**Widely accepted**	Freeze-fracture TEM of *Oocystis apiculate,* maize and pine (Brown & Montezinos, 1976; Haigler & Brown, 1986; Mueller & Brown, 1980)
2. Terminal complex arrangement facilitates the coalescence of glucan chains	TEM of green algae cell walls (Giddings, Brower, & Staehelin, 1980; Herth, 1983)	Partially confirmed: Conflicting evidence	Live-cell imaging of *Arabidopsis* cell walls and *in vitro* studies of cellulose synthesis (Cho et al., 2017; Li et al., 2016; Purushotham et al., 2016; Watanabe et al., 2015)
3. Cellulose is synthesized from terminal complexes	Sequencing analysis of the *Bcs* operon in *Acetobacter xylinum* and *CESA* genes in cotton (Pear et al., 1996; Saxena et al., 1990; Wong et al., 1990)	**Widely accepted**	Immunolabelling of CESA proteins in freeze fractured azuki bean complexes (Kimura et al., 1999)
4. CSCs are composed of a 'hexamer of hexamers' that synthesize cellulose microfibrils containing 36 chains	Hypothesis based on TEM structure (Herth, 1983)	Modified: Microfibrils consist of 18-24 chains. More evidence suggests the CSC is a hexamer of trimers, synthesizing an 18-chain microfibril.	Physical studies of microfibril widths in mung bean, freeze fracture of *Physcomitrella patens,* stoichiometry of *Arabidopsis* and *in vitro* trimer formation in poplar (Gonneau, Desprez, Guillot, Vernhettes, & Hofte, 2014; Hill et al., 2014; Newman & Hemmingson, 1990; Nixon et al., 2016; Vandavasi et al., 2016)
5. Each CESA protein synthesizes one glucan chain	CSC crystallography in *Rhodobacter sphaeroides* (Morgan et al., 2013)	Recent evidence: In *PttCesa8* homotrimers, each CESA particle associates with a single glucan molecule	Cryogenic-EM structure of *PttCesa8* homotrimers produced *in vitro* (Purushotham, Ho, & Zimmer, 2020)
6. Three distinct CESA isoforms are required for cellulose synthesis	CESA mutant analysis in *Arabidopsis* (Desprez et al., 2007; Taylor, Howells, Huttly, Vickers, & Turner, 2003)	Modified: Some cross-over between isoforms	Functional complementation in *Arabidopsis* (Carroll et al., 2012; Li, Lei, & Gu, 2013)
7. CESA proteins have 8 transmembrane domains	Sequencing analysis of *A. xylinum* and cotton (Pear et al., 1996; Saxena et al., 1990; Wong et al., 1990)	Modified: CESA proteins have 7 transmembrane domains	Mutational analysis and functional complementation in *Arabidopsis* and *P. patens* and structural analysis of *PttCESA8* homotrimers (Purushotham et al., 2020; Slabaugh et al., 2016)
8. CESA transmembrane domains form a channel for glucan chain release	CSC crystallography in *R. sphaeroides* (Morgan et al., 2013)	Recent evidence: In *PttCesa8* homotrimers, the transmembrane domains of each CESA particle forms a channel	Cryogenic-EM structure of *PttCesa8* homotrimers produced *in vitro* (Purushotham et al., 2020)
9. Cellulose microfibrils are extended by the stepwise addition of glucose	CSC crystallography in *R. sphaeroides* (Morgan et al., 2013)	*Not confirmed in plants*	
10. Microfibrils are simultaneously crystallized and polymerized	Calcofluor white interference in *A. xylinum* (Benziman, Haigler, Brown, White, & Cooper, 1980)	**Accepted with limited further study**	

11. The rosette structure promotes the crystallization of glucan chains	Hypothesis based on TEM structure (Herth, 1983)	**Accepted on little empirical evidence**	Mutational studies in *Arabidopsis* and poplar (Arioli et al., 1998; Harris et al., 2012; Purushotham et al., 2016)
12. Polymerization drives CSC movement	Observational (Herth, 1983)	**Widely accepted**	Live-cell imaging and biophysical modelling in *Arabidopsis* (Diotallevi & Mulder, 2007; Paredez, Somerville, & Ehrhardt, 2006)
13. Multi-net growth hypothesis	TEM of *Nitella* and *Tradescantia* (Roelofsen & Houwink, 1951)	*Not universally accepted*: Cannot explain anisotropy in all tissue types	AFM and FESEM in *Arabidopsis* (Marga, Grandbois, Cosgrove, & Baskin, 2005; Wiedemeier et al., 2002; Xin et al., 2020)
14. Alignment hypothesis	TEM and polarizing microscopy (Green, 1962; Ledbetter & Porter, 1963)	Partially confirmed: Not representative of all tissue types	Live-cell imaging in *Arabidopsis* (Himmelspach, Williamson, & Wasteneys, 2003; Paredez et al., 2006; Sugimoto, Himmelspach, Williamson, & Wasteneys, 2003)
15. Direct-guidance model	TEM and live-cell imaging in *Arabidopsis* (Heath, 1974; Paredez et al., 2006)	Updated: *CSI1*/*POM2* links CSCs with microtubules in primary cell walls	Y2H and *csi1/pom2* mutant analysis in *Arabidopsis* (Bringmann et al., 2012; Gu et al., 2010)
16. CSCs are assembled in the Golgi	TEM and freeze fracture of *Zinnia elegans* (Haigler & Brown, 1986)	In question: ER assembly has been proposed but evidence is scarce	Live-cell imaging in *Arabidopsis* (Gardiner, Taylor, & Turner, 2003; Paredez et al., 2006; Park, Song, Shen, & Ding, 2019)
17. Microtubules define CSC delivery	TEM of *Z. elegans* and *Coleus* (Haigler & Brown, 1986; Hepler & Newcomb, 1964)	Updated: Microtubules coincide with Golgi pausing events and the insertion of SmaCC/MASCs	Live-cell imaging in *Arabidopsis* (Crowell et al., 2009; Gutierrez, Lindeboom, Paredez, Emons, & Ehrhardt, 2009)
18. CSCs are recycled	Live-cell imaging and mutagenesis in *Arabidopsis* (Bashline, Li, Anderson, Lei, & Gu, 2013; Bashline, Li, Zhu, & Gu, 2015)	Partially confirmed: Evidence of CME, but it is not known if they are recycled	

Updated models now predict that CSCs that are composed of a hexamer of trimers or tetramers, producing 18- or 24-chain microfibrils, respectively (Table 1). SANS, WAXS and ssNMR examination of secondary cell walls in spruce and primary cell walls in celery collenchyma are consistent with a 24-chain model (Fernandes et al., 2011; Thomas et al., 2013) whereas an 18-chain model is favored in mung bean primary cell walls (Newman et al., 2013). Assuming all CESA proteins within a CSC are active, evidence from studies of *Arabidopsis* leans towards an 18-chain model, as equimolar concentrations of CESA proteins (Gonneau et al., 2014; Hill et al., 2014) and the formation of *CESA1* homotrimers in solution are both incompatible with a 24-chain model (Vandavasi et al., 2016). In *Arabidopsis*, models predict that CSCs composed of 18 CESA proteins contain either hetero or homo-trimers. Each lobe contains either three distinct or identical CESA isoforms, based on the 1:1:1 stoichiometry of CESA proteins, the formation of homotrimers *in vitro* and the requirement of three CESA isoforms for a functioning CSC *in vivo* (Figure 1A-B).

Due to the range of techniques, species and cell wall types adopted by different studies, it is hardly surprising that there is no consensus amongst research groups. It is also plausible that both the 18- and 24-chain model are correct under different circumstances, since microfibril diameters can vary (Martinez-Sanz, Pettolino, Flanagan, Gidley, & Gilbert, 2017). For example, in poplar tension wood, individual microfibrils are twice as wide in the G-layer compared to the adjacent secondary cell wall layers (Müller, Burghammer, & Sugiyama, 2006) and in fruit tissues, the microfibril diameter can be as low as 1 nm (Niimura, Yokoyama, Kimura, Matsumoto, & Kuga, 2009). Measuring the width of microfibrils and estimating the number of CESA proteins as a proxy for the number of glucan chains is not ideal, as microfibrils frequently interact with other matrix components and CESA proteins are not necessarily all active within a rosette. However, deciphering accurate CSC compositions in different cell walls and species may not be possible until CSCs and CESAs can be examined at higher resolution.

2.3 CSCs – Architecture

Discovering CESA proteins hugely expanded our capabilities for studying cellulose synthesis, as it became possible to identify CESA homologs by sequencing analysis in species where the complex had not been visualized. During this time, *Arabidopsis* had gained popularity as a molecular model and so became the preferred study system for cellulose synthesis. CESA homologs were successfully identified in *Arabidopsis* by screening mutant populations for cellulose deficiencies. CESA proteins were first described in the primary cell walls of the *radial swelling mutant*, *rsw1*, (Arioli et al., 1998) which exhibited stunted growth and reduced cellulose content at 31°C and in three *irregular xylem mutants*, *irx1/3/5,* exhibiting deformed secondary cell walls in vessels (Turner & Somerville, 1997). After the *Arabidopsis* genome was sequenced, a total of 10 CESA genes (*CESA1-10*) were identified (Richmond, 2000).

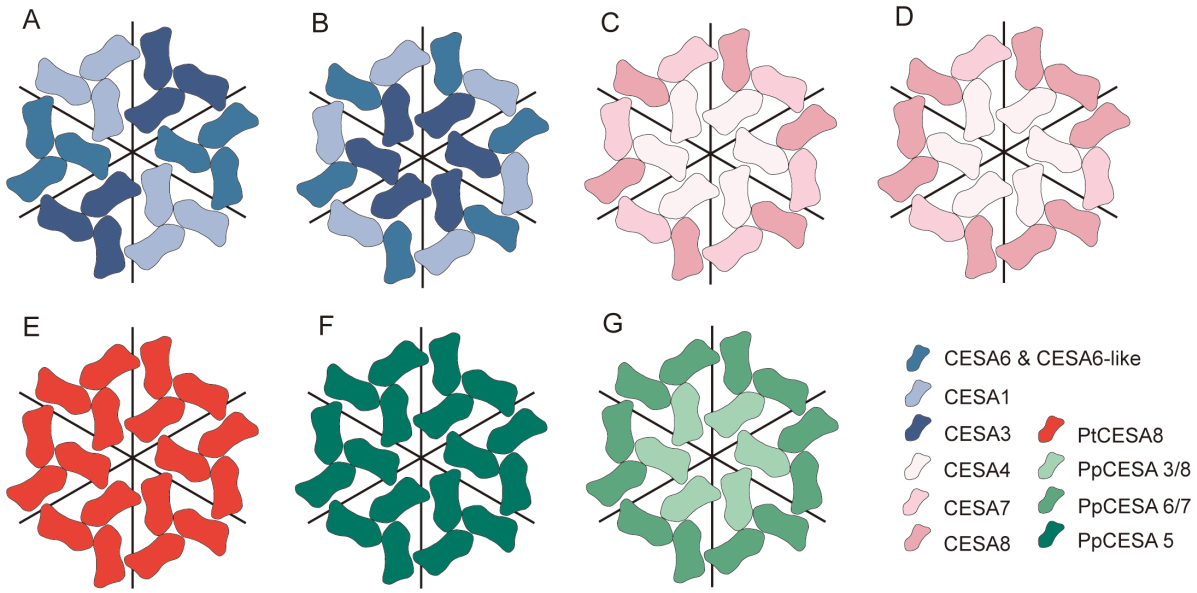

Figure 1 – Predicted arrangement of CESA proteins within the CSC. In *Arabidopsis* primary cell walls, CESA proteins exist as either (**A**) homotrimers or (**B**) heterotrimers within the CSC (Hill, Hammudi, & Tien, 2014). (**C**) Models of CSCs in the secondary cell walls of *Arabidopsis* and spruce predict that CESA proteins have a 1:1:1 stoichiometry (Zhang et al., 2018b). In the secondary cell walls of poplar, CSCs have a (**D**) 3:2:1 stoichiometry of *CESA8:4:7* in normal wood, and a (**E**) 8:3:1 stoichiometry in tension wood (Zhang et al., 2018b). Models of CSCs in *Physcomitrella patens* predict a (**F**) homo-oligomer composition of *PpCESA5* in primary cell walls (Goss, Brockmann, Bushoven, & Roberts, 2012) and a (**G**) hetero-trimer composition in secondary cell walls (Norris et al., 2017; Scavuzzo-Duggan et al., 2018).

With the identification of multiple CESAs, it was soon realized that CSCs were not made up of a homogenous population of CESA proteins. CESA proteins can be divided into two distinct families depending on the type of cell wall. In *Arabidopsis*, *CESA1*, *CESA3* and *CESA6*/*CESA6*-like proteins (*CESA2, CESA5, CESA9*) are required in the primary cell wall (Persson et al., 2007) and in secondary cell walls, *CESA4*, *CESA7* and *CESA8* are indispensable for plant growth (Taylor et al., 2003). Three distinct isoforms are required to form a functioning complex as individually mutating each of these CESA isoforms causes severe defects in cell wall synthesis (Desprez et al., 2007; Taylor et al., 2003). *CESA1* and *CESA3* are essential for primary cell wall synthesis because *cesa1* and *cesa3* mutants are gamete lethal, whereas *cesa6* mutants can still function due to partial redundancy with *CESA6*-like proteins, though they still exhibit a severe lack of cellulose and growth defects (Persson et al., 2007). Recent genetic work has shed uncertainty on the rigid distinction between primary and secondary cell wall CESAs, since primary cell wall CESAs can form functional complexes with secondary cell wall CESAs in both poplar and *Arabidopsis* (Carroll et al., 2012; Li et al., 2013; Song, Shen, & Li, 2010). Furthermore, primary cell wall CESAs can interact with secondary cell wall CESAs both *in vitro* and *in vivo*, and *pCESA7*::*CESA1* can partially rescue *cesa8* knock-outs (Carroll et al., 2012). *CESA6*-like proteins are also important in synthesizing specialized secondary cell walls, as cellulose defects are apparent in the seed coat of *cesa2*, *cesa5*, *cesa9* mutants and in the mucilage of *cesa5* mutants (Mendu et al., 2011). As cellulose synthesis is vital for plant growth, some promiscuity between *CESA* binding may exist to ensure cellulose production is maintained. Mixed complexes may represent 'intermediates' that facilitate the rapid changeover between primary and secondary cell wall synthesis. Whether functional compatibility between CESA isoforms is merely due to the high conservation between CESA catalytic domains is uncertain, as currently there is no evidence these mixed complexes are formed *in vivo.*

It is not known why the composition of CESAs in the CSC differs between primary and secondary cell walls, but it must be essential to warrant such a significant energy investment in the changeover of CESA isoforms between cell wall types. The ability of single CESA isoforms to synthesize cellulose causes further confusion as to why multiple isoforms are needed (Purushotham et al., 2016). Only 25% of the microfibrils produced *in vitro* are crystalline, so perhaps microfibrils synthesized in the absence of other CESAs are structurally defective. Differences between the composition of the CSC in primary and secondary cell walls is ultimately driven by evolution, since the common ancestor of moss and seed plants exhibited a rosette-CSC comprised of a single CESA isoform (Roberts & Bushoven, 2007). Both moss and seed plants evolved two classes of CESA proteins independently, stressing that a variety of isoforms evolved to fulfil separate functions in different cellular environments and under different regulatory pathways. In *P. patens*, *PpCESA5* is required for primary cell wall formation in leaf gametophores (Figure 1F), whereas *PpCESA3/8* and *PpCESA6/7* are required for secondary cell wall deposition in stereids that resemble tracheary elements (Figure 1G). Convergent evolution of hetero-oligomeric CSCs suggests that the specialization of CESA was a fundamental requirement for synthesizing cellulose under different *in vivo* conditions (Li et al., 2019).

Attempts to tease apart the different functions of CESA by systematic mutagenesis have demonstrated that while their precise functions are not fully understood, CESAs clearly impart unequal roles in cellulose synthesis. Mutating catalytic motifs in different CESA proteins differentially impacts cellulose synthesis indicating CESA proteins vary in their catalytic ability. For instance, a *cesa8* mutant exhibits severe reductions in cellulose content, whereas only mild decreases are reported for *cesa4* (Kumar, Atanassov, & Turner, 2017). A popular hypothesis is that CESA isoforms may determine crystallinity because secondary cell walls contain a higher proportion of crystalline cellulose than primary cell walls. In particular, *CESA8* may be fundamental for mediating crystallinity, as not only does is it appear more catalytically active than other isoforms in the CSC (Kumar et al., 2017), but it is more abundant than *CESA4* and *CESA7* in poplar secondary cell walls that have a high degree of crystallinity (Zhang et al., 2018b). In *Arabidopsis* and Norway spruce, CESA proteins are expressed in equimolar concentrations with a stoichiometry of 1:1:1 (Figure 1C). However, in poplar the stoichiometry of *CESA8:4:7* is 3:2:1 (Figure 1D) (Zhang et al., 2018b). In poplar tension wood, a significant increase in *PtCESA8b* mRNA transcripts produces a more exaggerated shift in stoichiometry of 8:3:1 that coincides with cellulose that is almost completely crystalline (Figure 1E) (Zhang et al., 2018b). Interestingly, *PtCESA7* transcripts do not change in abundance and *PtCESA4* and *PtCESA8a* decreases, indicating different CESA isoforms confer different roles in tension wood.

In higher plants, CESA proteins have 8 transmembrane domains separated by a large catalytic cytosolic loop between the 2nd and 3rd domain. The 8 transmembrane domain model has recently been challenged by Slabaugh et al. (2016) who proposed that the 5th domain is an interfacial helix, making CESA a 7 transmembrane domain protein (Table 1). The absence of this transmembrane domain relocates a loop with a conserved FxVTxK motif to the cytoplasm. Here, it might assist in substrate binding as it does in its bacterial counterpart. Based on the crystal structure of the BcsA-BcsB complex, the transmembrane domains of CESA proteins are predicted to form a channel through which newly synthesized glucan chains are released (Morgan et al., 2013). Recent structural analysis of *PttCESA8* homotrimers indicates that the transmembrane domains of each CESA forms a continuous channel across the membrane, similar to the bacterial complex (Purushotham et al., 2020). Furthermore, these channels appear to converge in the center of the trimer to facilitate the secretion and coalescence of nascent glucan chains, suggesting higher plant CESAs and the BcsA-BcsB complex share a common mechanism for cellulose synthesis.

In CESA proteins, the catalytic domain contains the highly conserved motifs (D, D, DxxD and QxxRW) common to all GT2 enzymes (Sethaphong et al., 2013). Point mutations in these motifs in *Arabidopsis* and cotton have verified that they perform distinct roles in catalysis and substrate binding. The first two aspartates (D, D) are involved in the binding of UDP-glucose substrates, DxxD acts as a base for glucan chain extension and the QxxRW motif as a binding site for the final glucan residues in the chain (Saxena, Brown, & Dandekar, 2001). Within the catalytic loop there is a plant-conserved region (P-CR) between D and DxxD and a hypervariable region (HVR) at the other end of the domain (Pear et al., 1996). The HVR contains a class-specific region (CSR) specific to each isoform that is widely homologous between different species, yet highly diverse amongst different isoforms (Vergara & Carpita, 2001). Intuitively, the CSR is thought to determine CESA isoform specificity. However, chimeric studies in *Arabidopsis* and moss have firmly established that the CSR is largely interchangeable between different CESA isoforms. Swapping domains between different CESA proteins does not compromise catalytic ability and chimeric CESA proteins can successfully rescue the corresponding mutants, indicating that class specificity is neither restricted, nor defined by these regions (Hill, Hill, Roberts, Haigler, & Tien, 2018; Kumar et al., 2017; Scavuzzo-Duggan et al., 2018; Sethaphong et al., 2016; Wang, Howles, Cork, Birch, & Williamson, 2006).

Alternatively, the CSR and P-CR are speculated to mediate CESA interactions, CESA positioning in the CSC and rosette formation, since both these regions are absent from bacteria that do not form rosettes. Indeed, when CSR and P-CR regions are included in structural models of the CESA catalytic domain, they diverge significantly from the structure of *Bcs* (Olek et al., 2014; Purushotham et al., 2016). Studies combining mathematical modelling with low-resolution SANS and SAXS analysis provide conflicting evidence for the roles of P-CR and CSR in CSC formation. In rice, the CSR region is predicted to assist in *OsCESA8* dimerization and the P-CR region is implicated in dimer-dimer interactions (Olek et al., 2014), whereas in *Arabidopsis*, the P-CR region of *AtCESA1* is predicted to recruit non-CESA proteins and the CSR is implicated in trimer-trimer assembly (Vandavasi et al., 2016). Resolving the crystal structure of the P-CR region in *OsCESA8* revealed that it consists of two α-helices linked by a large extended loop (Rushton et al., 2017). Incorporating the crystal structure into previous SAXS-based models predicts that the P-CR is located in the catalytic core close to the active site (Rushton et al., 2017), which is easily reconciled with the dimerization of CESA proteins (Olek et al., 2014). Discrepancy between dimer- and trimer-models is likely caused by a low homology of CSR between different isoforms and the purification of CESA isoforms under different experimental conditions. As these studies report the formation of homodimers and homotrimers from single CESA isoforms *in vitro*, it cannot be discounted that hetero-dimers and -trimers may be formed in the presence of other CESA proteins *in vivo* due to the high conservation of catalytic domains. While the precise role of P-CR and CSR in CSC assembly is ambiguous, it can be concluded that these regions mediate CESA interactions in different capacities.

The N-terminal contains a zinc-finger domain that can dimerize with the same or different CESA proteins under redox conditions in cotton (Kurek, Kawagoe, Jacob-Wilk, Doblin, & Delmer, 2002). A recent study of the *Arabidopsis* acylome revealed that the zinc-finger is likely to be inactive in *CESA4* and *CESA8* since the acylation of key cysteine residues compromise its ability for metal ion binding (Kumar, Carr, & Turner, 2020). On the contrary, mutating key cysteines in the zinc-finger of *CESA7* greatly impairs its function, suggesting *CESA7* may be essential for maintaining the integrity of the CSC (Kumar et al., 2020). With more intricate examination of CESA structures, the exact functions of CESA domains and individual CESA isoforms in the CSC are starting to unravel.

Continuing advancements in sequencing technology have facilitated the identification of CESA homologs in a huge diversity of eukaryotes and prokaryotes. Assigning function to CESA homologs

represents the rate-limiting step as functional genetic analysis can take years in some species, particularly trees. Expression analysis has been used as an indirect indicator of CESA function in various tissues and points of development. However functional genomics is needed to definitively assign function to these orthologs. So far this has been achieved in several commercially important species such as rice, maize, poplar and eucalyptus. Further quantification is needed, particularly in woody species that have multiple copies of CESA isoforms that presumably have distinct roles in wood formation (Zhang et al., 2018b).

2.4 Crystallization and polymerization

Due to the lability of cellulose I, it was reasoned that crystallization and polymerization must be co-ordinated for cellulose I to acquire stability in the cell wall (Saxena & Brown, 2005). Inhibiting crystallization with Calcofluor white in *A. xylinum* increases the rate of polymerization by four-fold, suggesting that not only are these processes tightly coupled, but that crystallization limits polymerization (Benziman et al., 1980). In *R. sphaeroides,* newly synthesized glucan chains are elongated by the stepwise addition of glucose units (Morgan et al., 2016) - a mechanism thought to be shared with plants (Table 1). In higher plants, the close proximity of rosette subunits likely facilitates simultaneous crystallization with the coalescence of glucan chains (Table 1), since the loss of CSC organization is often concurrent with an increase in amorphous cellulose. For example, mutating the catalytic subunit or transmembrane domains of *AtCESA*s decreases crystalline cellulose (Arioli et al., 1998; Harris et al., 2012) and removing the zinc-finger domain in *pttcesa8* mutants produces amorphous cellulose exclusively, reinforcing that the structure of the rosette is mandatory for crystallization (Purushotham et al., 2016).

Continuous chain elongation was predicted to drive the movement of CSCs through the plasma membrane (Herth, 1983) (Table 1). A later study also suggested that the continuous synthesis of cellulose from CSCs generates the driving force to propel its movement, based on the migration of *YFP::CESA6* in the plasma membrane observed with spinning disc confocal microscopy (Paredez et al., 2006). Biophysical modelling of CSC movement based on crystallization and polymerization alone, predicted that the CSC could move in the plasma membrane at a speed of 10^{-9} – 10^{-8} m s^{-1} (Diotallevi & Mulder, 2007), similar to reported values of 5-8 x 10^{-9} m s^{-1} (Paredez et al., 2006).

2.5 Non-catalytic genes involved in cellulose synthesis

Identifying non-catalytic genes essential for cellulose synthesis was relatively straightforward in bacterial genomes, where functionally related genes often cluster together. For plants that have more complex genomes, candidates were initially identified using forward genetic screens with cellulose biosynthesis inhibitors. One of the first non-CESA genes to be identified was the putative membrane-spanning endo-1,4 β-D-glucanase, *KORRIGAN* (*KOR1*) (Nicol et al., 1998). Determining the precise role of *KOR1* has not been possible, because mutating *KOR1* causes a range of phenotypes including reduced crystalline cellulose (Maloney & Mansfield, 2010); altered CSC velocity (Vain et al., 2014); and perturbed microfibril orientation (Lei et al., 2014). Since the evolution of *KOR1* pre-dates the appearance of CESA in green algae, *KOR1* may have been fully responsible for synthesizing cellulose in primitive life forms (Lampugnani et al., 2019). As *KOR1* is still functional in higher plants it must have had a selective advantage, possibly by assisting with cellulose synthesis in conjunction with CESA proteins. With the exception of *CESA7*, *KOR1* can bind to all cell wall CESA proteins in yeast two hybrid (Y2H) assays (Mansoori et al., 2014) and fluorescent tagging of *KOR1* revealed that it associates with CSCs in the Golgi, TGN, secretory vesicles and the plasma membrane (Lei et al., 2014; Vain et al., 2014). Together, this strongly indicates that *KOR1* is a permanent resident of the CSC that modulates CSC function throughout its lifespan. Due to its tight association with the CSC, defects observed in *kor1* mutants may be an indirect consequence of gene perturbation, further

complicating the assignment of *KOR1* function. Another early non-CESA gene identified was the glycosyl-phosphatidyl inositol–anchored protein, *COBRA (COB)* (Benfey et al., 1993; Roudier et al., 2005). *COB* has been described as a 'scaffold' for maintaining microfibril orientation and binding in *Arabidopsis* (Roudier et al., 2005). *COB* evolved alongside CESA, coinciding with the shift in linear arrays to rosette-shaped CSCs (Lampugnani et al., 2019), and therefore may be important in synthesizing glucan chains in close proximity to one another.

Significant advancements in genetic techniques have now made it possible to identify genetic candidates based on their physical interactions with CSC machinery. Many CESA-interacting proteins have been discovered from Y2H assays, GFP-TRAP, co-immunoprecipitation combined with mass-spectrometry, *in vitro* pull downs and biomolecular fluorescence complementation (BiFC). In particular, key proteins integral for maintaining the relationship between CSC and underlying microtubules have been described including, *CELLULOSE SYNTHASE MICROTUBULE UNCOUPLING PROTEIN* (*CMU*) that prevents the lateral displacement of microtubules from the hypothesized pressure generated by CSC migration (Liu et al., 2016); *CELLULOSE-SYNTHASE INTERACTIVE PROTEIN 1* (*CSI1/POM2*) that links CSCs with microtubules and marks regions for CSC exocytosis (Bringmann et al., 2012; Gu et al., 2010; Zhu, Li, Pan, Xin, & Gu, 2018); and *COMPANION OF CELLULOSE SYNTHASE* (*CC*) that promotes microtubule dynamics for CSC localization under specific stress conditions (Endler et al., 2015). *CMU, CSI1* and *CC* were some of the most recent cellulose-related genes to evolve, appearing in a group of *Charophyceae* algae known as *Zygnematophyrae* (Lampugnani et al., 2019). The evolution of a specialized microtubule band involved in cytokinesis in *Zygnematophyrae* strongly suggests that *CMU*, *CSI1* and *CC* evolved for the succinct co-ordination of microfibrils and microtubules – a feature that was retained by higher plants (Lampugnani et al., 2019).

In general, the roles of non-catalytic proteins in cellulose synthesis have been described in the context of primary cell walls. However, there is increasing evidence that many of these genes have reciprocal or divergent functions in secondary cell walls. For instance, *kor1* mutants exhibit defects in vessel secondary cell wall formation in *Arabidopsis* (Szyjanowicz et al., 2004) and *KOR1* can physically interact with secondary cell wall CESAs (Mansoori et al., 2014; Vain et al., 2014). The role of *CSI1* in secondary cell walls is disputed (Zhu, Xin, & Gu, 2019). No cellulose defects are apparent in *csi1* mutants (Gu et al., 2010), yet it is abundant in induced *Arabidopsis* tracheary elements (Derbyshire et al., 2015) and in *pom2-4* mutants, xylem vessels have irregular wall patterns and *CESA7* is mis-aligned with microtubules (Schneider et al., 2017). An alternative isoform of *COB, COBL4,* may be specifically involved in producing highly crystalline cellulose in secondary cell walls. *COBL4* is upregulated in secondary cell walls (Brown, Zeef, Ellis, Goodacre, & Turner, 2005) and tension wood (Andersson-Gunneråas et al., 2006) and the *COBL4* homolog in rice, *BRITTLE CULM1 (bcl),* can bind to crystalline microfibrils (Liu et al., 2013). As many non-catalytic genes clearly participate in various aspects of both primary and secondary cell wall formation, perhaps assigning precise functions is not possible or biologically accurate.

2.6 Biochemistry of cellulose synthesis

Studying the biochemical aspects of cellulose synthesis has been notoriously problematic over the last 30 years. A persistent problem has been that β-1,3 linked callose was preferentially synthesized over β-1,4 linked cellulose from plant membrane extracts, hampering efficient cellulose production (Amor, Haigler, Johnson, Wainscott, & Delmer, 1995). Moderate improvements were achieved from *in vitro* cultures of hybrid aspen that produced almost 50% cellulose (Ohlsson et al., 2006) and microsome preparations of blackberries that yielded up to 1 mg cellulose (Lai-Kee-Him et al., 2002), but poor yields and callose contamination were still major concerns. Significant advances have recently been achieved from the heterologous expression of CESA isoforms from poplar and *P.*

patens in yeast (Cho et al., 2017; Purushotham et al., 2016). Reconstituting *PttCESA8* and *PpCESA5* in proteoliposomes that mimic the lipid bi-layer environment proved essential for successful synthesis, as disrupting the bilayer with detergent eliminated catalytic activity. Radio-active tracing of UDP-[^{3}H]-Glc, determined that catalysis was maintained for 90-150 minutes, a considerable improvement from previous *in vitro* reactions that terminated after 10 minutes (Amor et al., 1995). Whether these cellulose microfibrils are representative of microfibrils *in vivo* presents the next major challenge.

Despite significant advancements in the synthesis of cellulose *in vitro*, the purification and reconstitution of the entire CSC has so far not been possible and remains a major research priority. Biochemical inferences of CESAs have been made from low resolution SAXS analysis that does not depend on protein crystallization and comparisons with the crystal structure of the BcsA-BcsB complex. Recent structural analysis of a *PttCESA8* homotrimer with cryogenic-EM suggested that plants and bacteria share a common mechanism for synthesizing cellulose (Purushotham et al., 2020). However, this mechanism may not be entirely indicative of CSC function in higher plants since it has not been established if these homotrimers exist *in vivo*. Furthermore, the cellulose microfibrils produced by recombinant *PttCESA8* homotrimers expressed in insect cells, do not resemble microfibrils produced by previous *in vitro* assays or microfibrils synthesized *in vivo*. Microfibrils were 40 times narrower (10-15 Å) than the 4.3 and 4.8 nm wide microfibrils produced by re-constituted *PttCESA8* and *PpCESA5* proteoliposomes (Cho et al., 2017; Purushotham et al., 2016), and microfibrils were amorphous, contrary to higher plants that contain a high proportion of crystalline cellulose. Whilst heterologous expression of CESAs in different systems may be the cause of this discrepancy, inconsistencies in the *in vitro* cellulose production of *PttCESA8* casts some doubt on the proposed mechanism of *PttCESA8* homotrimers. Nonetheless, the ability to study the structure of purified CESAs with cryogenic-EM, represents a major breakthrough in the study of CSC structure (Table 1) that will facilitate a more complete understanding of cellulose synthesis in the future.

3. When is cellulose synthesized?

Plant growth and shape is achieved predominately by cell expansion as opposed to cell division (McFarlane, Doring, & Persson, 2014). Cell expansion is permitted by internal stresses generated by turgor pressure and the slow yielding of the primary cell wall (Cosgrove, 2016). Unsurprisingly, the organization of cellulose microfibrils and the cell wall architecture is tightly linked with cell expansion. Early hypotheses regarding the role of cellulose microfibrils in cell expansion were developed solely from TEM-based observations. While TEM is a useful tool for visualizing the cell wall architecture in its entirety, sample preparation can disrupt native cell wall structures. Developing techniques that preserve the cell wall architecture with higher fidelity, such as field emission scanning electron microscopy (FESEM) and AFM, meant that these predictions could be more rigorously scrutinized, but only in the innermost cell wall layer. Cell expansion studies have been fairly limited to cell-types with thin cell walls, which lend themselves to high resolution imaging, particularly the epidermal tissues from onion (Suslov, Verbelen, & Vissenberg, 2009) and the dark-grown hypocotyl and root elongation zone from *Arabidopsis*.

3.1 Cell elongation and expansion

Directional growth in plant cells is achieved by anisotropic expansion, whereby cells stretch longitudinally and undergo minimal lateral expansion. As the load bearing structure, cellulose microfibrils are important in generating differential resistance to turgor pressure and determining the direction of growth. Consequently, anisotropic expansion is highly reliant on efficient cellulose biosynthesis. In fact, many cellulosic biosynthetic genes were initially identified from mutants exhibiting abnormal cell elongation, such as *cesa1^{rsw1}* (Arioli et al., 1998); *cesa6$^{prc1\text{-}1}$* (Fagard et al., 2000); *cob* (Benfey et al., 1993); *kor1* (Nicol et al., 1998); and *pom1/2* (Hauser, Morikami, & Benfey,

1995). For some mutants, including *cesa6*$^{prc1\text{-}1}$ and *pom1*, the microfibril deposition is not altered (Baskin, 2005; Pagant et al., 2002; Refregier, Pelletier, Jaillard, & Hofte, 2004) meaning these defects in anisotropic expansion may be a knock-on effect of cellulose perturbation caused by hormonal changes or compensational responses of other cell wall components.

Cellulose microfibrils was first connected with anisotropic growth from TEM-based observations of the primary cell walls of *Tradescantia* stamen hairs (Roelofsen & Houwink, 1951). In the newly formed central lamellae, cellulose microfibrils were deposited perpendicular to the direction of cell growth, whereas new lamellae deposited towards the outside of the cell tended to have a longitudinal orientation, parallel to the growth axis. Changes in microfibril orientation led to the concept of 'multi-net growth' (Table 1). Under the multi-net growth hypothesis, the progressive re-alignment of microfibrils towards the outer cell layers causes the cell to elongate (Roelofsen & Houwink, 1953). Identical observations were subsequently reported in algae (Tsekos, 1999) and *Arabidopsis* (Anderson et al., 2010). The transverse orientation of microfibrils was predicted to generate differential resistance to turgor pressure by physically restricting lateral expansion and promoting rapid longitudinal elongation (Green, 1960, 1962).

The multi-net growth hypothesis is one of the longest standing hypotheses in cellulose biosynthesis, but it has lost considerable backing as many of the conditions required by the multi-net growth hypothesis are no longer satisfied when complex tissues of higher plants are considered (Table 1). This is particularly true of cross polylamellate walls in the epidermis of hypocotyls, stems and coleoptiles that exhibit parallel microfibrils that alternate by 30-90° between successive lamellae (Chan et al., 2010; Zhang et al., 2016a). Furthermore, transverse microfibril orientation does not consistently induce anisotropy (Wiedemeier et al., 2002; Xin et al., 2020) and expansion can be achieved without the passive reorientation of microfibrils (Bashline, Lei, Li, & Gu, 2014; Marga et al., 2005). In the stem and hypocotyl epidermis, cell elongation is achieved despite having longitudinally or randomly orientated microfibrils. To explain this discrepancy, it has been suggested that the inner cell layers control the direction of expansion by imparting the necessary axial force to the outer epidermis (Baskin, 2005), or by generating sufficient anisotropic expansion than negates the isotropic expansion of the epidermis (Fujita et al., 2011). Indeed, examining the innermost cell wall layer of etiolated *Arabidopsis* hypocotyls with FESEM demonstrated that the transverse microfibril orientation of the inner regions could induce growth anisotropy of the outer epidermal layers (Chan et al., 2011; Crowell et al., 2011). Additionally, Baskin (2005) discovered that anisotropic expansion was reduced when microfibril alignment was not uniform within tissues, suggesting that the net alignment of microfibrils between cells is more crucial than within cells for determining the degree of anisotropic expansion. It is important to note that hypotheses regarding cell expansion are predominately tested in model systems and are unlikely to be representative of other cell types and developmental stages that differ in their extent of expansion, due to differences in turgor pressure and microfibril orientation.

3.2 Relationship with microtubules

In early studies of cellulose synthesis, one of the most frequent observations made was the relationship between cellulose microfibril orientation and cortical microtubules patterns (Hepler & Newcomb, 1964). 'Cortical cytoplasmic elements', later realized to be microtubules, were proposed to guide the positioning of nascent cellulose microfibrils (Green, 1962). Based on the parallel alignments of cortical microtubules with cellulose microfibrils, the 'alignment hypothesis' was developed (Ledbetter & Porter, 1963) (Table 1). The complementary association between microtubules and microfibrils was initially confirmed in TEM studies of green algae (Tsekos, 1999), and later by confocal microscopy, where *YFP::CESA6* and *RFP::TUA6* signals co-localized in the

plasma membrane of *Arabidopsis* primary cell walls (Li et al., 2016; Paredez et al., 2006). Early studies showed that disrupting microtubule dynamics prevented cell elongation, providing a direct link between microfibril orientation and microtubules (Morejohn, 1991). Live-cell imaging provided further confirmation that CSCs are directly guided by underlying cortical microtubules, by demonstrating that the trajectories of CSCs and newly synthesized microfibrils were re-orientated to align with new patterns of microtubules, following microtubule disruption (Paredez et al., 2006).

Whilst many studies largely support the alignment model, there are some notable inconsistencies. It was soon realized that the relationship is not as simple as when first proposed since microtubules are not ubiquitously required for the alignment of CSCs and microfibrils (Chan & Coen, 2020; Mizuta & Okuda, 1987). In the innermost layers of the root and hypocotyl epidermis, the parallel trajectories of CSCs and the transverse orientations of cellulose microfibrils are maintained in the absence or disorder of microtubules (Himmelspach et al., 2003; Sugimoto et al., 2003; Xin et al., 2020), suggesting that microfibril assembly is not reliant on microtubules. Under these circumstances, CSCs that are not linked with underlying microtubules may maintain their alignments by tracking previous microtubule trajectories, as observed with light microscopy (Chan & Coen, 2020). Alternatively, microtubules may influence cell expansion and cellulose synthesis by determining the extent of cellulose crystallinity. When cell expansion is stimulated at 29°C, the proportion of crystalline cellulose simultaneously decreases, however when the abundance of microtubules is reduced in the temperature-sensitive *mor1-1* mutant, cells can no longer expand and cellulose crystallinity content does not change at 29°C (Fujita et al., 2011). Microtubules may modulate crystallinity by controlling the fluidity of the plasma membrane or the interaction with non-cellulosic components (Fujita, Lechner, Barton, Overall, & Wasteneys, 2012). It is also true that cellulose microfibrils may determine the distribution of cortical microtubules. Tobacco BY2 cells and *Arabidopsis* roots treated with cellulose biosynthesis inhibitors exhibit a dispersed, unordered microtubule array (Fisher & Cyr, 1998; Himmelspach et al., 2003) and in *cesa2* and *cesa6* mutants' cortical microtubules have a distorted alignment (Chu et al., 2007; Paredez, Persson, Ehrhardt, & Somerville, 2008). A bi-directional interaction between microtubules and microfibrils is not necessarily incompatible with the alignment hypothesis, but it indicates that revisions need to be made. A more suitable model may be the 'cellulose-constraint' model proposed by Giddings and Staehelin (1991) whereby cortical microtubules constrain paths for CSC movement and cellulose microfibrils exert biophysical forces on cortical microtubules as part of a self-reinforcing feedback loop.

The next step in understanding the relationship between microtubules and microfibrils was to establish the basis of their association. Whilst live-cell imaging confirms that their trajectories are correlated, it does not indicate whether CSC and microtubules are in direct contact, or if other factors are involved. Heath (1974) proposed the popular 'direct guidance model', whereby CSCs directly interact with microtubules (Table 1). Genetic evidence now supports that CSCs indirectly interact with microtubules through a linker protein known as *CSI1* (Gu et al., 2010; Li, Lei, Yingling, & Gu, 2015). *CSI1* interacts with both microtubules and the catalytic domain of CESA proteins *in vitro* and *RFP::CSI1* co-localizes with *YFP::CESA6 in vivo* (Bringmann et al., 2012; Gu et al., 2010; Li, Lei, Somerville, & Gu, 2012). In *csi1-1* mutants, CSC trajectories are uncoupled from microtubules and CSC velocity is slower (Gu et al., 2010; Li et al., 2012), although when microtubules are removed, CSCs can maintain ordered trajectories. This may be explained if *CSI1* is essential for the initial alignment of microtubules with CSCs, after which the trajectory does not depend on microtubule presence (Schneider et al., 2017). *CC1* also directly interacts with microtubules and the CSC. Mutating two tyrosine residues essential for microtubule-binding in the *CC1* gene, disrupts the parallel alignment between CSCs and microtubules, suggesting *CC1* has an important role in

maintaining the relationship between CSCs and microtubules (Kesten et al., 2019). A wealth of studies has convincingly demonstrated that CSCs and microtubules are co-dependent and both are important for cell anisotropy. Ultimately our ideas match those originally proposed by Green (1962), but the relationship is clearly more nuanced than first proposed and so these early hypotheses have been more rigorously scrutinized.

4. CSC trafficking

A huge breakthrough that facilitated the study of CSC trafficking was the development of live-cell imaging that allowed CSC dynamics to be visualized within the cell. Functional complementation of the non-lethal *cesa6*$^{prc1\text{-}1}$ mutant, with fluorescently tagged *CESA6* proteins, enabled CSC movements in primary cell walls to be traced with confocal microscopy (Paredez et al., 2006). Studies are preferentially performed on dark-grown *Arabidopsis* hypocotyls, due to the high abundance of CSCs coupled with thin primary cell walls that enhance imaging resolution. On the other hand, high quality imaging of CSC movements in secondary cell walls, which can be deeply embedded within tissues, has been a much greater challenge. With the development of inducible lines, it is now possible to visualize tracheary elements with greater resolution (Yamaguchi et al., 2010). Together with live-cell imaging, proteomic analysis has been ground-breaking in identifying key proteins that interact with CSCs during trafficking.

4.1 CSC assembly

Terminal complex assembly was hypothesized to occur in either the ER or the Golgi, before being transported to the plasma membrane (Table 1). Evidence for Golgi assembly was first indicated from TEM-based observations of fully formed terminal complexes embedded in the Golgi, TGN and post-Golgi vesicles in algae (Brown, Franke, Kleinig, Falk, & Sitte, 1970; Giddings et al., 1980). For algal species that produce large linear complexes, such as *Erthyrocladia* and *Vaucheria*, assembly is partially completed at the membrane as vesicles containing single particles, multi-subunits and precursor-complexes all fuse with the membrane (Mizuta & Brown, 1992; Tsekos, 1999). In multicellular organisms, rosettes were first observed in the TGN and post-Golgi vesicles in differentiating tracheary elements of *Zinnia elegans* mesophyll cells (Haigler & Brown, 1986).

Little progress has been made in uncovering how the CSC assembles, due to the difficulties in visualizing pre-Golgi processes, particularly in the ER. During live-cell imaging, *YFP::CESA* fluorescence is either very weak or undetectable in the ER (Crowell et al., 2009; Gutierrez et al., 2009; Paredez et al., 2006), presumably due to the quenching of fluorescence deeper in the cell. In the *cesa6*^{D395N} mutant, diffuse signals of *YFP::CESA6* below the Golgi was interpreted as the retention of malformed CSCs in the ER (Park et al., 2019). However, as no ER marker was used, and the distribution of *CESA1* and *CESA3* was not examined in conjunction with *CESA6,* it is not possible to differentiate whether the entire CSC or single *CESA6* proteins are retained in the ER (Park et al., 2019). In secondary cell walls, the co-localization of *GFP::CESA4* and *GFP::CESA8* with the ER binding protein, BiP, in *cesa7*^{irx3} mutants further supports the idea that incomplete CSCs cannot be transported from the ER (Gardiner et al., 2003). Despite the limited evidence, it is generally accepted that CSCs are assembled in the ER where they would undergo quality control (Strasser, 2018). Dissecting specific molecular partners in CSC assembly in the ER is problematic, as ER-secreted proteins rely on a set of shared molecular chaperons for folding, so mutating these genes will likely exert pleiotropic effects unrelated to cellulose synthesis.

Assembled CSCs are assumed to be transported via direct streaming or in COPII vesicles to the Golgi where they are then modified before export (Neumann, Brandizzi, & Hawes, 2003). One study on *Arabidopsis* has indicated that CSCs may assemble in the Golgi with the assistance of Golgi-localized

STELLO proteins (*STL1/2*) that have a glycosyltransferase (GT) domain. In *stl1 stl2* double mutants, primary and secondary CSCs were less abundant, CSC delivery rates were reduced and *CESA3* distribution was altered in the Golgi (Zhang et al., 2016b), which are all phenotypes consistent with defective Golgi assembly. Split-ubiquitin and BiFC assays confirmed that *STL1* and *STL2* could bind to all primary and secondary cell wall CESAs, but whether the precise interactions involve the *STELLO* GT domain was not tested (Zhang et al., 2016b). CSC assembly may also be facilitated by *KOR1* and *COB* that co-localize with CESA proteins in the Golgi (Lei et al., 2014; Roudier et al., 2005; Vain et al., 2014), however, this has not been functionally assessed. Identifying how CESA proteins interact with accessory proteins in the Golgi or ER will fill in some of the crucial gaps in our understanding of CSC assembly.

4.2 CSC delivery

Although progress on CSC assembly has been slow, considerable knowledge has been gained in the trafficking of CSCs to the plasma membrane (Figure 2). Early observations of intact CSCs in the Golgi and TGN/EE (Giddings et al., 1980; Haigler & Brown, 1986) were later reinforced by live-cell imaging of fluorescent CESA particles in the Golgi and TGN/EE (Crowell et al., 2009; Paredez et al., 2006). Therefore, trafficking of the CSC to the plasma membrane may occur from the Golgi via the TGN, or independently from the Golgi. The main route for CSC delivery is thought to occur via the Golgi, as various TGN markers, *VHA-a1* and *SYP61,* do not co-localize with CSC membrane insertion events (Crowell et al., 2009). However, confirming this is problematic since the TGN/EE acts as both a secretory and recycling organelle, harbouring populations of both newly synthesized and recycled CSCs (Viotti et al., 2010). Two types of CSC trafficking vesicles have been identified depending on their microtubule associations: small cellulose synthase compartments (SmaCCs) (Gutierrez et al., 2009) and microtubule associated SmaCCs (MASCs) (Crowell et al., 2009). Partial co-localization of SmaCCs/MASCs with TGN/EE molecular markers implicates SmaCCs/MASCs in both the secretion of *de novo* synthesized CSCs, and CSC internalisation. In general, SmaCCs/MASCs are regarded as endocytotic vesicles, though it has become evident that they confer multiple roles in CSC trafficking, complicating their study.

CSC delivery was observed in early TEM observations whereby vesicles containing terminal complexes frequently coincided with cortical microtubules underlying cell wall thickenings (Haigler & Brown, 1986; Hepler & Newcomb, 1964). Live-cell imaging of *CESA3* and *CESA6* with tubulin further corroborated the tight overlap between cortical microtubules and CSC delivery events in primary cell walls (Crowell et al., 2009; Gutierrez et al., 2009). Microtubules mark specific sites for CSC delivery as disrupting intact microtubules networks causes the random insertion of SmaCCs/MASCs into the membrane (Gutierrez et al., 2009; Paredez et al., 2006), and newly delivered CSCs track microtubule arrays after photo bleaching (Crowell et al., 2009). CSC insertion into the plasma membrane also coincides with Golgi pausing events immediately beneath sites of cortical microtubules (Crowell et al., 2009), implicating the Golgi in mediating CSC delivery. Although microtubule distribution also coincides with sites of secondary cell wall deposition in developing vessels, removing microtubules does not influence Golgi pausing events in the delivery of *CESA7* (Wightman & Turner, 2008). Instead, transverse actin defines CSC delivery sites and actin cables indirectly transport CSCs to the plasma membrane, since actin depolymerization prevents CSC delivery and halts Golgi movement of CSCs (Wightman & Turner, 2008). While actin is not required for CSC insertion in primary cell walls (Sampathkumar et al., 2013), it may play a role in delivering CSCs to the membrane, as disrupting actin polymerization causes *CESA3* and *CESA6* Golgi bodies to aggregate beneath the membrane (Crowell et al., 2009; Gutierrez et al., 2009). Microtubules and actin involvement in CSC delivery may be spatially separated because subcortical SmaCCs have reduced velocity when actin cables were disrupted (Gutierrez et al., 2009). In the subcortical regions, actin may be responsible for the

678 movement of the Golgi to sites of microtubules in the cell cortex that define domains for secretion.
679 Recently, the actin-based motor protein, myosin *XI*, was implicated in the trafficking of CSCs in
680 primary cell walls (Figure 2). In triple *xi1 xi2 xi3* mutants and wild-type plants treated with myosin
681 inhibitors, CSC delivery is reduced and vesicles containing CSC vesicles accumulate below the
682 membrane (Zhang, Cai, & Staiger, 2019). Failed delivery was attributed to defective vesicle tethering
683 and fusion due to the overlap of *XI* with *CESA6* fluorescent signals near the membrane. Whether this
684 is an indirect effect of defective Golgi pausing is unclear.

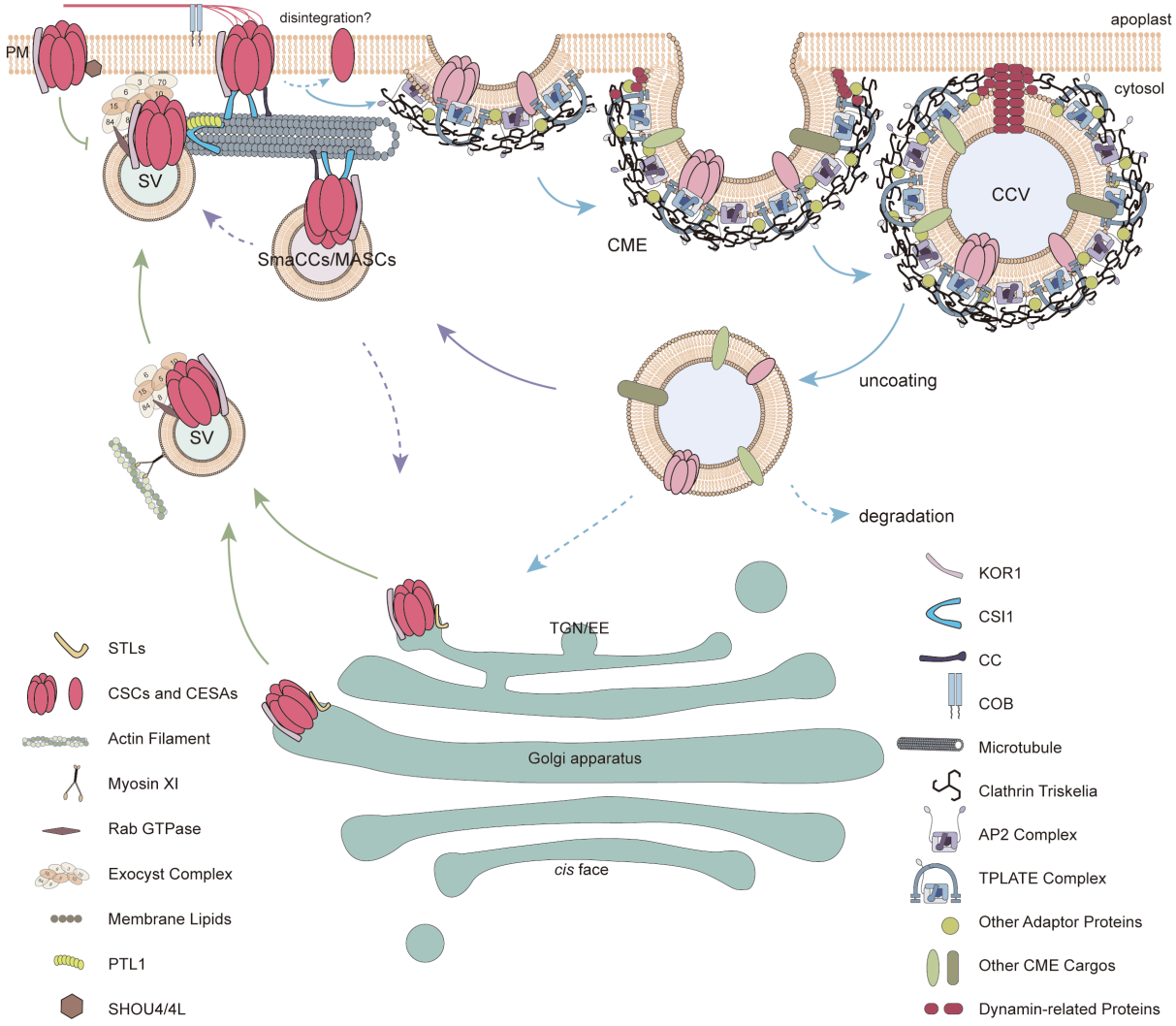

Figure 2 – A model of CSC trafficking in primary cell walls. CSC assembly is predicted to occur in the Golgi, with the help of Golgi-localized *STELLO* (*STLs*) proteins. CSCs are then transported from the TGN/EE and the Golgi via secretory vesicles (SV) and are delivered to specific sites on the plasma membrane that are marked by *CSI1* proteins linked to microtubules. Myosin XI may also help deliver SV containing CSCs to the plasma membrane along actin filaments. Physical interactions between *PATROL1* (PTL1) and the exocyst complex with SVs are required for the insertion of CSCs into the plasma membrane. *SHOU4/4L* negatively regulates CSC delivery. Various non-CESA proteins are required for optimal cellulose biosynthesis, including *COB* and *CC* that associate with CSCs at the plasma membrane and *KOR1* that additionally associates with the CSC during trafficking. Intact or degraded CSCs can be internalized into clathrin-coated vesicles (CCV) and undergo clathrin-mediated endocytosis (CME). Various CME components, such as the adaptor protein 2 complex (AP2), TPLATE complex are essential for CME. Internalized CSCs can be recycled back to the plasma membrane via SmaCCs/MASCs.

Trafficking of any protein complex relies on four key phases - vesicle budding, cytosolic transport, tethering and ultimately fusion with the destination membrane. From studies on bacteria, yeast and animals it is obvious that delivery is co-ordinated by a complex interplay of proteins. Key players that have been identified include, Rab GTPases that target vesicles towards the destination membrane and mediate the fusion of the two membranes; tethering factors such as soluble *N*-ethylmaleimide-sensitive factor attachment protein receptor (SNAREs) that assist with fusion; and the exocyst complex. Identifying candidates specific for CSC trafficking has been challenging due to the vast genetic redundancies of these families in *Arabidopsis,* combined with the fact that Rab GTPases and SNAREs associate with multiple cargoes (Uemura et al., 2012; Vernoud, Horton, Yang, & Nielsen, 2003). Some candidates have been identified, including the Golgi-localized Rab-H1B, whereby *CESA6* has reduced motility and impaired exocytosis in loss of function mutants (He et al., 2018). However, their direct involvement in CSC trafficking has not been clear. Co-purification of *CESA6* with the syntaxin *SYP61,* a sub-family of SNAREs, implicated *SYP61* vesicles in the tethering of *CESA6* to the membrane (Drakakaki et al., 2012). However, as *SYP61* is a major component of post-Golgi vesicles it is unlikely to be specific for CSC trafficking. Ideally the purification of CESA specific compartments such as SmaCCs/MASCs would provide more insight into CSC delivery. However, due to their small size and low fluorescence signal this may prove difficult unless aggregated populations are extracted. Furthermore, extracting SmaCCs/MASCs during different points of CSC trafficking may be informative of the different genetic components involved in recycling and delivery, allowing the identification of specific markers of these processes.

Unsurprisingly, the precise temporal and spatial insertion of CSCs into the membrane is under tight genetic control. Co-immunoprecipitation of *CSI1* identified several genetic components that assist with CSC delivery in primary cell walls (Figure 2), including *PATROL 1* (*PTL1*) and the exocyst subunits, *SEC5B* and *SEC10* (Zhu et al., 2018). Mutagenesis combined with *in vitro* pull downs demonstrated that CSC delivery relies on intricate physical interactions between *CESA6, CSI1*, *PTL1* and exocyst subunits. A model was developed for CSC delivery by carefully examining the temporal and spatial localization of these proteins during a live-cell imaging time-course (Zhu et al., 2018). *CSI1* defines the domain in the plasma membrane for delivery and possibly acts as a direct tether of SmaCCs to the membrane, since SmaCC formation is reliant on the interaction between *CSI1* and microtubules (Lei et al., 2015). After *CSI1* interacts with the vesicle, *PTL1* primes the vesicle for fusion by subunits of the exocyst complex, *SEC5B* and *SEC10*, that complete fusion. The association of *PTL1* is fleeting but essential, as delivery rates are slower in *ptl1,* and *ptl1 csi1* double mutants have an additive phenotype. Whether this mechanism is shared by secondary cell walls has not yet been established, although the accumulation of exocyst subunits and *CSI1* during secondary cell wall deposition indicates that this could be a strong possibility (Derbyshire et al., 2015). Recently, *SHOU4* proteins were identified as negatively regulators of CSC exocytosis (Polko et al., 2018). In *shou4 shou4l* double mutants enhanced CSC delivery is evident from an elevated density of *CESA6* at the plasma membrane and an increase in amorphous cellulose content (Polko et al., 2018). Direct binding of the cytoplasmic domain of *SHOU4* proteins with the catalytic domains of primary cell wall CESAs may cause the retention of CSCs in the cytoplasm, though this is speculative at present.

4.3 CSC endocytosis and recycling

The population of CSCs at the plasma membrane at any given time is determined by a balance between exocytosis and endocytosis and is often used as a proxy for the rate of cellulose synthesis. How this interplay is regulated is unknown, but it is possible that the plasma membrane can monitor the density of CSC and subsequently mediate CSC delivery and recycling as part of a self-regulating feedback system. Supporting evidence has been provided from *rabh1b* CSC trafficking mutants that are defective in both exocytosis and endocytosis, suggesting that the two processes are inter-

dependent (He et al., 2018). CSC recycling is inherently difficult to quantify, but it is widely believed to be a dominant process for several reasons. Firstly, CSCs have an average longevity of 30 minutes (Jacob-Wilk, Kurek, Hogan, & Delmer, 2006), yet typically, CSC membrane lifespan is only 7 - 8 minutes (Sampathkumar et al., 2013) suggesting CSC may be recycled several times before they are degraded. Secondly, as CSCs are large protein complexes, repeatedly constructing CSCs every 7 minutes would exert huge energetic costs on the cell. Finally, SmaCC/MASC populations tend to accumulate in cells not actively synthesizing cellulose, or cells under osmotic stress (Crowell et al., 2009; Gutierrez et al., 2009). In adverse conditions, SmaCCs/MASCs may accumulate underneath the membrane as a 'temporary store' of CSCs that are rapidly recycled back once stress is alleviated. Furthermore, when protein and cellulose synthesis is inhibited, *CESA3* accumulates in MASCs within 7 minutes suggesting internalisation is more likely than *de novo* secretion (Gutierrez et al., 2009).

Clathrin-mediated endocytosis (CME) is a dominant process in Eukaryotes but it is only in the last two decades that its importance has been appreciated in plants (Holstein, 2002; Reynolds, Wang, Pan, & Bednarek, 2018). Clathrin coated vesicles were first observed in the TGN in the 1980s (Coleman, Evans, & Hawes, 1988) and 30 years later they were shown to be integral for CSC internalisation (Figure 2). Two components of CME machinery, *AP2M* and *TWD40-2*, have been implicated in CSC endocytosis (Bashline et al., 2013; Bashline et al., 2015). *AP2M* is homologous with a medium subunit of the adaptor protein complex 2 (*AP2*) that assists with docking and recruiting CME machinery (Bashline et al., 2013) and *TWD40-2* is a potential member of a TPLATE complex (TPC) that is unique to plants (Gadeyne et al., 2014). In *ap2m* and *twd40-2* mutants, reductions in endocytosis were inversely correlated with a higher density of CSC at the membrane (Bashline et al., 2013; Bashline et al., 2015). Co-operation of *TWD40-2* with *AP2M* is required for CME, as not only do they directly interact, but reductions in endocytosis and cellulose content are exacerbated in *ap2m twd40-2* double mutants (Bashline et al., 2015). However, they may confer distinct roles in CME, since hypocotyls exhibit reduced elongation in *twd40-2* but have increased elongation in *ap2m.* *TWD40-2* also has a much longer lifespan than *AP2M* during CME so it may be involved in scission from the membrane or quality control. Another TPC subunit, *TML*, can also interact with *CESA6* catalytic units. *tml* knock-down lines exhibit similar decreases in cellulose content and an increased population of CSC at the membrane that is not attributable to increased delivery rates (Sanchez-Rodriguez et al., 2018). CME represents one route of CSC endocytosis, as SmaCCs/MASCs abundance is reduced, but not completely abolished in *ap2m* mutants (Lei et al., 2015). The TPLATE may have evolved to specifically tailor CME in plants or mediate endocytosis independently, so continued study of this complex will be revealing about CSC endocytosis.

CESAs have been described as *AP2M* cargo because *AP2M* can bind to *CESA6* and *CESA3* in split-ubiquitin assays and *in vitro* pull downs, and *mCHERRY::CESA6* patterns overlap with *YFP::AP2M* (Bashline et al., 2013). But discrepancies in their physical dimensions questions whether CSC can be internalized by CME, as the catalytic core of CSCs is 50% wider than the lumen of typical CME particles (Bashline, Li, & Gu, 2014; Li et al., 2014). De-constructed complexes may be internalized as an increased number of CSC particles at the membrane coupled with decreased cellulose content in *twd40-2* mutants indicates CSC breakdown may start prior to internalisation (Bashline et al., 2015). CSCs readily form monomers, dimers and trimers in solution under a range of conditions suggesting that CSCs may be easily broken down *in vivo* by local alterations in the membrane environment (Atanassov, Pittman, & Turner, 2009; Olek et al., 2014; Vandavasi et al., 2016). Alternatively, CSCs may appear larger if it is bound to other components that may be released prior to endocytosis.

Whether endocytosed CSCs destined for proteolysis are trafficked to the vacuole directly or go via the TGN/EE is unclear, as both seem plausible (Crowell et al., 2009). Likewise, it is not known

whether SmaCCs go to the TGN/EE before re-inserting CSCs into the membrane or bypass the TGN/EE altogether. At least some recycled CSCs pass through the TGN/EE as poor acidification of the TGN/EE in *det3* mutants causes defects in both secretion and recycling (Luo et al., 2015). As the TGN/EE is a sorting hub it would be convenient if all internalized CSCs travelled to the TGN/EE and were then exported for either recycling or degradation. Differentiating between populations of newly synthesized and recycled proteins that cross-over at the TGN/EE is a taxing question and has impeded research in this area. Determining the protein composition of vesicles involved at each stage of CSC trafficking may reveal markers that signify the destination of the vesicle, alleviating this problem. During the rapid changeover between primary and secondary cell wall synthesis, CSC exocytosis and endocytosis are temporally separated briefly, so could be probed to answer some of these outstanding questions. At the onset of secondary cell wall deposition in inducible *VND7* tracheary elements, the *tdTomato::CESA6* signal decreases in the membrane and increases at the Golgi, representing recently endocytosed primary cell wall CSCs. Once *YFP::CESA7* starts appearing at the Golgi, the *tdTomato::CESA6* signal disappears from the Golgi and a diffuse signal re-appears in the vacuole, indicating that the recently endocytosed *tdTomato::CESA6* are transported to the vacuole during secondary cell wall deposition (Watanabe et al., 2018).

5.How is cellulose synthesis regulated?

Probing the molecular regulation of cellulose synthesis has only been possible in the last 20 years, due to significant advances in the generation of genetic mutants, genetic constructs, and next generation sequencing technologies. High-throughput sequencing has been used to explore the regulation of cellulose synthesis at multiple aspects including, genomic (DNA), transcriptional (mRNA), translational (proteins), and post translational processes (metabolites and small RNA), causing a marked shift in research focus from structural to molecular studies.

5.1 Transcriptional regulation

Since all cells have a primary cell wall and cells are continuously made throughout development, genes involved in primary cell wall synthesis are ubiquitously expressed (Hamann et al., 2004). As such, transcriptional regulators are likely to be housekeeping genes that are not specific for cellulose synthesis. Potential candidates have been identified in the *ETHYLENE-RESPONSE-FACTOR* (*ERF*) IIId and IIIe transcription factor family. Overexpressing *ERF35* produces thick cell walls with a primary cell wall composition in *nst1 nst3* mutants that lack secondary cell walls (Sakamoto et al., 2018). Since many *ERF* transcription factors are co-expressed with *CESA1, CESA3* and *CESA6,* and *ERF34-ERF43* can physically bind to the promoters of primary cell wall CESA genes, the *ERF* transcription factor family may have a central role in regulating cellulose deposition in primary cell walls (Saelim et al., 2019; Sakamoto et al., 2018). Additionally, a brassinosteroid responsive transcription factor, *BES1,* can increase CESA expression by binding to the E-box (CANNTG) element in the promoters of *CESA1*, *CESA3* and *CESA6* (Xie, Yang, & Wang, 2011). However, *BES1* is unlikely to be a specific activator of primary CESAs, as *BES1* can simultaneously induce *CESA4* and *CESA8* expression.

In contrast to primary cell walls, the transcriptional network responsible for regulating cellulose synthesis during secondary cell wall formation has been extensively characterized in *Arabidopsis* (Yamaguchi et al., 2010; Zhong, Lee, Zhou, McCarthy, & Ye, 2008) and it is functionally conserved in woody species (Zhang, Xie, Tuskan, Muchero, & Chen, 2018a) and grasses (Rao & Dixon, 2018). Two main transcription factor families containing either NAC- or MYB domains, co-ordinate the expression of CESA biosynthetic genes. The NAC transcription factors, *NAC SECONDARY WALL THICKENING PROMOTING FACTORS (NST1/2)* and *SECONDARY WALL-ASSOCIATED NAC DOMAIN PROTEIN (SND1)* can activate cellulose synthesis in fibers, with *snd1 nst1* double mutants exhibiting reduced cellulose content and impaired secondary cell wall formation (Zhong, Richardson, & Ye,

2007). NAC-domain transcription factors activate two downstream transcription factors, *MYB46* and *MYB83*, which are functionally redundant and *MYB103* (Zhong et al., 2008). *MYB103* can activate the expression of GUS reporter genes driven by the *CESA8* promoter, implicating *MYB103* as a specific regulator of cellulose deposition (Zhong et al., 2008). In cellulose-rich cotton fibers, *MYB103* is one of the first transcription factors that is expressed during the changeover between primary and secondary cell wall deposition, providing further support that it is an important regulator of cellulose synthesis (MacMillan et al., 2017). Overexpressing *MYB46* and *MYB83* causes an increase in *CESA* expression that is accompanied by excessive cellulose deposition in ectopic cell walls, implicating *MYB46/83* as direct activators of cellulose synthesis (Ko, Kim, & Han, 2009; McCarthy, Zhong, & Ye, 2009). *MYB46* can specifically regulate CESA expression by binding to 8-bp *MYB46*-responsive *cis* regulatory elements (M46RE) in CESA promoters (Kim et al., 2013b). Introducing CESA genes with point mutations in the M46RE into *cesa* mutants could not restore cellulose synthesis, demonstrating that *MYB46* binding is crucial for regulating cellulose synthesis in *Arabidopsis* (Kim, Kim, Ko, Kim, & Han, 2013a). Other direct targets of *MYB46* include the CCCH zinc finger genes, *C3H14* and *C3H15* (Ko et al., 2009), which cause ectopic deposition of cellulose and upregulate CESA genes when overexpressed (Chai et al., 2015). More recently other transcription factor families have been implicated in cellulose synthesis regulation, such as *WRKY* and *ERF*. Cellulose deposition is stimulated in *wrky12* mutants (Wang et al., 2010) or when the *ERF* transcription factor, *PdSHINE2*, is overexpressed in tobacco (Liu et al., 2017).

5.2 Post-translational regulation

Constitutive expression of CESA genes in primary cell walls implies that post-transcriptional regulation may be more important for regulating cellulose synthesis (Hamann et al., 2004). Arguably, the best studied form of post-translational regulation is phosphorylation (Speicher, Li, & Wallace, 2018). Phosphoproteomic analysis of primary CESA proteins demonstrated that many sites in the N-terminus and HVR of the central loop contain conserved serine (S) and threonine (T) residues that have the potential to be phosphorylated (Durek, Schudoma, Weckwerth, Selbig, & Walther, 2009; Nuhse, Stensballe, Jensen, & Peck, 2004). The effects of phosphorylation were first examined by mutating S and T sites to alanine (A) that eliminates phosphorylation, or glutamine (E) that mimics phosphorylation. Inhibiting phosphorylation at $T^{166}A$, $S^{686}A$ and $S^{688}A$ residues in the HVR of *cesa1*^{rsw1} mutants produced a variety of cellulose defective phenotypes, including reduced cellulose content, poor anisotropic cell expansion, reduced CSC velocity and the loss of bi-directional movement, which were all rescued when phosphorylation was restored (Chen, Ehrhardt, & Somerville, 2010). In contrast, permitting phosphorylation at $S^{162}E$, $T^{165}E$ and $S^{167}E$ in *cesa1*^{rsw1} mutants caused cellulose defective phenotypes, indicating that a balance between de-phosphorylation and phosphorylation finely tunes the regulation of *CESA1* (Chen et al., 2010). Removing microtubules with oryzalin rescued the velocity and bi-directional movement of *CESA1* at the membrane, supporting the idea that the phosphorylation of CESA proteins may modulate microfibril synthesis and anisotropic growth by its interaction with microtubules (Chen et al., 2010). Similar studies on *CESA3* and *CESA5* have reinforced that phosphorylation is critical for cellulose synthesis regulation in primary cell walls. For example, phosphorylation of $S^{211}A$ and de-phosphorylation of $T^{212}E$ of *CESA3* is crucial for maintaining anisotropy, deposition, bundling and bi-directional microtubule-based motility at the membrane (Chen et al., 2016) and phosphorylating *CESA5* alters the migration of CSC in a phytochrome dependent manner (Bischoff et al., 2011). Phosphorylation may also be important for mediating CESA endocytosis in the secondary cell wall since *in vitro* phosphorylation of *CESA7* causes its degradation via the proteosome (Taylor, 2007). Identifying the corresponding protein kinases that activate phosphorylation has proved troublesome, with conflicting evidence in the literature and large genetic redundancies in kinase families (McFarlane et al., 2014). In Arabidopsis, the protein

kinase *BRASSINOSTEROID INSENSITIVE 2 (BIN2*) can phosphorylate a *CESA1* peptide, *CESA1*^{T157}, *in vitro* (Sanchez-Rodriguez et al., 2017). In *cesa1 bin2-1* double mutants, the CSC moves significantly faster at the membrane, implicating *BIN2* as a negative regulator of cellulose synthesis in the primary cell wall (Sanchez-Rodriguez et al., 2017). *BIN2* phosphorylation impacts the activity of the entire CSC, even though it cannot phosphorylate *CESA3* or *CESA6* peptides, demonstrating the importance of phosphorylation as a regulatory mechanism.

More recently it was revealed that secondary cell wall CESAs are heavily modified by the attachment of the fatty acid palmitate at conserved cysteine residues, also known as S-acylation. Mutating four cysteines in the VR2 and two cysteines in the C-terminal domain of *CESA7* prevented the trafficking of *CESA7* to the plasma membrane from the Golgi (Kumar et al., 2016). The role of S-acylation may be broadened to include other aspects of cellulose biosynthesis, since many important non-CESA proteins such as *KOR1; CMU; CC; SHOU; PTL1;* and CME components are also acylated (Kumar et al., 2020). Furthermore, heavy S-acylation of *CESA3* and *CSI1* suggests S-acylation may function in primary cell walls (Kumar et al., 2020; Kumar et al., 2016). Although many of these assumptions have not been yet been functionally tested, it is probable that S-acylation is a dominant regulator of post-translational processes that we have only just begun to understand.

6. Significant achievements and future directions

Remarkably, many of the original hypotheses that were based on simple TEM observations and X-ray diffraction patterns in bacteria and algae, have stood the test of time and have been verified in higher plants by using a range of more accurate techniques (Table 1). Although, re-visiting other long-standing hypotheses with more sensitive techniques has revealed that some concepts are too simplistic to account for the diversity in cell wall architecture. Most notably the multi-net growth hypothesis is insufficient to explain anisotropy in all conditions and the relationship between CSCs and microtubules is not universally coupled. Significant progress in our capacities to study cellulose synthesis *in vivo* with live-cell imaging, AFM, FESEM and molecular genetics has resulted in some drastic changes in our understanding of some key aspects of cellulose synthesis, and in some cases has divided research groups. In the last 10 years, the 36-glucan chain model has been disregarded in favor of an 18-24 chain model, new models of cell elongation have been proposed and even the classic 8 transmembrane CESA-model has been brought into question (Table 1). While *Arabidopsis* has proved an invaluable model for enhancing our understanding of cellulose synthesis, these results need to be approached with caution as this system may not be representative of higher plants in general. Broadening the sample types may help settle variable findings between research groups and will strengthen the validity of hypotheses across higher plants. With many unanswered or modified hypotheses still requiring verification (Table 1), we can expect many great discoveries and changes in the field during this century. Adopting multidisciplinary strategies that link together the biophysical and biochemical properties of cellulose with underlying genetics and cell wall architecture, will be fundamental for this venture. Successful purification of CSCs, imaging the entire CSC *in situ* and assigning functions to microfibril properties are arguably the next major breakthroughs on the agenda in order to advance the study of cellulose synthesis, as such fundamental knowledge will be critical to eventually manipulate cellulose synthesis for desired use.

Acknowledgements

H.A. and Y.G. were supported by National Science Foundation Grant 1951007. D.W. was supported by the Center for LignoCellulose Structure and Formation, an Energy Frontier Research Center funded by the Department of Energy, Office of Science, Basic Energy Sciences under Award DESC0001090. S.L. was supported by startup funds from the Department of Biochemistry and Molecular Biology at Pennsylvania State University.

References

Amor, Y., Haigler, C. H., Johnson, S., Wainscott, M., & Delmer, D. P. (1995). A membrane-associated form of sucrose synthase and its potential role in synthesis of cellulose and callose in plants. *Proc Natl Acad Sci U S A, 92*(20), 9353-9357. doi:10.1073/pnas.92.20.9353

Anderson, C. T., Carroll, A., Akhmetova, L., & Somerville, C. (2010). Real-time imaging of cellulose reorientation during cell wall expansion in Arabidopsis roots. *Plant Physiol, 152*(2), 787-796. doi:10.1104/pp.109.150128

Andersson-Gunnerås, S., Mellerowicz, E., Love, J., Segerman, B., Ohmiya, Y., Coutinho, P., . . . Sundberg, B. (2006). Biosynthesis of cellulose-enriched tension wood in *Populus*: global analysis of transcripts and metabolites identifies biochemical and developmental regulators in secondary wall biosynthesis. *Plant Journal, 45*(2), 144-165. doi:10.1111/j.1365-313X.2005.02584.x

Arioli, T., Peng, L., Betzner, A. S., Burn, J., Wittke, W., Herth, W., . . . Williamson, R. E. (1998). Molecular analysis of cellulose biosynthesis in Arabidopsis. *Science, 279*(5351), 717-720. doi:10.1126/science.279.5351.717

Atalla, R. H., & Vanderhart, D. L. (1984). Native cellulose: a composite of two distinct crystalline forms. *Science, 223*(4633), 283-285. doi:10.1126/science.223.4633.283

Atanassov, II, Pittman, J. K., & Turner, S. R. (2009). Elucidating the mechanisms of assembly and subunit interaction of the cellulose synthase complex of Arabidopsis secondary cell walls. *J Biol Chem, 284*(6), 3833-3841. doi:10.1074/jbc.M807456200

Bashline, L., Lei, L., Li, S., & Gu, Y. (2014). Cell wall, cytoskeleton, and cell expansion in higher plants. *Mol Plant, 7*(4), 586-600. doi:10.1093/mp/ssu018

Bashline, L., Li, S., Anderson, C. T., Lei, L., & Gu, Y. (2013). The endocytosis of cellulose synthase in Arabidopsis is dependent on mu2, a clathrin-mediated endocytosis adaptin. *Plant Physiol, 163*(1), 150-160. doi:10.1104/pp.113.221234

Bashline, L., Li, S., & Gu, Y. (2014). The trafficking of the cellulose synthase complex in higher plants. *Ann Bot, 114*(6), 1059-1067. doi:10.1093/aob/mcu040

Bashline, L., Li, S., Zhu, X., & Gu, Y. (2015). The TWD40-2 protein and the AP2 complex cooperate in the clathrin-mediated endocytosis of cellulose synthase to regulate cellulose biosynthesis. *Proc Natl Acad Sci U S A, 112*(41), 12870-12875. doi:10.1073/pnas.1509292112

Baskin, T. I. (2005). Anisotropic expansion of the plant cell wall. *Annu Rev Cell Dev Biol, 21*, 203-222. doi:10.1146/annurev.cellbio.20.082503.103053

Benfey, P. N., Linstead, P. J., Roberts, K., Schiefelbein, J. W., Hauser, M. T., & Aeschbacher, R. A. (1993). Root Development in Arabidopsis: Four Mutants With Dramatically Altered Root Morphogenesis *Development, 119*(1), 57-70.

Benziman, M., Haigler, C. H., Brown, R. M., White, A. R., & Cooper, K. M. (1980). Cellulose biogenesis: Polymerization and crystallization are coupled processes in Acetobacter xylinum. *Proc Natl Acad Sci U S A, 77*(11), 6678-6682. doi:10.1073/pnas.77.11.6678

Bischoff, V., Desprez, T., Mouille, G., Vernhettes, S., Gonneau, M., & Hofte, H. (2011). Phytochrome regulation of cellulose synthesis in Arabidopsis. *Curr Biol, 21*(21), 1822-1827. doi:10.1016/j.cub.2011.09.026

Bowling, A. J., & Brown, R. M., Jr. (2008). The cytoplasmic domain of the cellulose-synthesizing complex in vascular plants. *Protoplasma, 233*(1-2), 115-127. doi:10.1007/s00709-008-0302-2

Brett, C. (2000). Cellulose microfibrils in plants: biosynthesis, deposition, and integration into the cell wall. *International Review of Cytology, 199*, 161-199. doi:10.1016/s0074-7696(00)99004-1

Bringmann, M., Li, E., Sampathkumar, A., Kocabek, T., Hauser, M. T., & Persson, S. (2012). POM-POM2/cellulose synthase interacting1 is essential for the functional association of cellulose synthase and microtubules in Arabidopsis. *Plant Cell, 24*(1), 163-177. doi:10.1105/tpc.111.093575

983 Brown, D. M., Zeef, L., Ellis, J., Goodacre, R., & Turner, S. (2005). Identification of novel genes in
984 Arabidopsis involved in secondary cell wall formation using expression profiling and reverse
985 genetics. *Plant Cell, 17*(8), 2281-2295. doi:10.1105/tpc.105.031542
986 Brown, R. (1996). The Biosynthesis of Cellulose. *Journal of Macromolecular Science - Pure and*
987 *Applied Chemistry, 33*(10), 1345-1373. doi:10.1080/10601329608014912
988 Brown, R., & Montezinos, D. (1976). Cellulose microfibrils: visualization of biosynthetic and orienting
989 complexes in association with the plasma membrane. *Proc Natl Acad Sci U S A, 73*(1), 143-
990 147. doi:10.1073/pnas.73.1.143
991 Brown, R. J., Franke, W. W., Kleinig, H., Falk, H., & Sitte, P. (1970). Scale formation in chrysophycean
992 algae. I. Cellulosic and noncellulosic wall components made by the Golgi apparatus. *J Cell*
993 *Biol, 45*(2), 246-271. doi:10.1083/jcb.45.2.246
994 Brown, R. M. J., & Saxena, I. M. (2000). Cellulose biosynthesis: A model for understanding the
995 assembly of biopolymers. *Plant Physiology and Biochemistry, 38*(1-2), 57-67.
996 doi:doi.org/10.1016/S0981-9428(00)00168-6
997 Carroll, A., Mansoori, N., Li, S., Lei, L., Vernhettes, S., Visser, R. G., . . . Trindade, L. M. (2012).
998 Complexes with mixed primary and secondary cellulose synthases are functional in
999 Arabidopsis plants. *Plant Physiol, 160*(2), 726-737. doi:10.1104/pp.112.199208
1000 Chai, G. H., Kong, Y. Z., Zhu, M., Yu, L., Qi, G., Tang, X. F., . . . Zhou, G. K. (2015). Arabidopsis C3H14
1001 and C3H15 have overlapping roles in the regulation of secondary wall thickening and anther
1002 development. *Journal of Experimental Botany, 66*(9), 2595-2609. doi:10.1093/jxb/erv060
1003 Chan, J., & Coen, E. (2020). Interaction between Autonomous and Microtubule Guidance Systems
1004 Controls Cellulose Synthase Trajectories. *Curr Biol, 30*(5), 941-947 e942.
1005 doi:10.1016/j.cub.2019.12.066
1006 Chan, J., Crowell, E., Eder, M., Calder, G., Bunnewell, S., Findlay, K., . . . Lloyd, C. (2010). The rotation
1007 of cellulose synthase trajectories is microtubule dependent and influences the texture of
1008 epidermal cell walls in Arabidopsis hypocotyls. *J Cell Sci, 123*(Pt 20), 3490-3495.
1009 doi:10.1242/jcs.074641
1010 Chan, J., Eder, M., Crowell, E. F., Hampson, J., Calder, G., & Lloyd, C. (2011). Microtubules and CESA
1011 tracks at the inner epidermal wall align independently of those on the outer wall of light-
1012 grown Arabidopsis hypocotyls. *J Cell Sci, 124*(Pt 7), 1088-1094. doi:10.1242/jcs.086702
1013 Chen, S., Ehrhardt, D. W., & Somerville, C. R. (2010). Mutations of cellulose synthase (CESA1)
1014 phosphorylation sites modulate anisotropic cell expansion and bidirectional mobility of
1015 cellulose synthase. *Proc Natl Acad Sci U S A, 107*(40), 17188-17193.
1016 doi:10.1073/pnas.1012348107
1017 Chen, S., Jia, H., Zhao, H., Liu, D., Liu, Y., Liu, B., . . . Somerville, C. R. (2016). Anisotropic Cell
1018 Expansion Is Affected through the Bidirectional Mobility of Cellulose Synthase Complexes
1019 and Phosphorylation at Two Critical Residues on CESA3. *Plant Physiol, 171*(1), 242-250.
1020 doi:10.1104/pp.15.01874
1021 Cho, S. H., Purushotham, P., Fang, C., Maranas, C., Diaz-Moreno, S. M., Bulone, V., . . . Nixon, B. T.
1022 (2017). Synthesis and Self-Assembly of Cellulose Microfibrils from Reconstituted Cellulose
1023 Synthase. *Plant Physiol, 175*(1), 146-156. doi:10.1104/pp.17.00619
1024 Chu, Z., Chen, H., Zhang, Y., Zhang, Z., Zheng, N., Yin, B., . . . Xie, Q. (2007). Knockout of the AtCESA2
1025 gene affects microtubule orientation and causes abnormal cell expansion in Arabidopsis.
1026 *Plant Physiol, 143*(1), 213-224. doi:10.1104/pp.106.088393
1027 Coleman, J., Evans, D., & Hawes, C. (1988). Plant coated vesicles. *Plant, Cell and Environment, 11*(8),
1028 669-684. doi:10.1111/j.1365-3040.1988.tb01150.x
1029 Cosgrove, D. J. (2016). Plant cell wall extensibility: connecting plant cell growth with cell wall
1030 structure, mechanics, and the action of wall-modifying enzymes. *J Exp Bot, 67*(2), 463-476.
1031 doi:10.1093/jxb/erv511
1032 Cosgrove, D. J., & Jarvis, M. C. (2012). Comparative structure and biomechanics of plant primary and
1033 secondary cell walls. *Front Plant Sci, 3*, 204. doi:10.3389/fpls.2012.00204

1034 Cousins, S. K., & Brown, R. M. (1997). X-ray diffraction and ultrastructural analyses of dye-altered
1035 celluloses support van der Waals forces as the initial step in cellulose crystallization.
1036 *Polymer, 38*(4), 897-902. doi:10.1016/s0032-3861(96)00589-7
1037 Crowell, E. F., Bischoff, V., Desprez, T., Rolland, A., Stierhof, Y. D., Schumacher, K., . . . Vernhettes, S.
1038 (2009). Pausing of Golgi bodies on microtubules regulates secretion of cellulose synthase
1039 complexes in Arabidopsis. *Plant Cell, 21*(4), 1141-1154. doi:10.1105/tpc.108.065334
1040 Crowell, E. F., Timpano, H., Desprez, T., Franssen-Verheijen, T., Emons, A. M., Hofte, H., &
1041 Vernhettes, S. (2011). Differential regulation of cellulose orientation at the inner and outer
1042 face of epidermal cells in the Arabidopsis hypocotyl. *Plant Cell, 23*(7), 2592-2605.
1043 doi:10.1105/tpc.111.087338
1044 Delmer, D. P. (1999). CELLULOSE BIOSYNTHESIS: Exciting Times for A Difficult Field of Study. *Annu*
1045 *Rev Plant Physiol Plant Mol Biol, 50*, 245-276. doi:10.1146/annurev.arplant.50.1.245
1046 Derbyshire, P., Menard, D., Green, P., Saalbach, G., Buschmann, H., Lloyd, C. W., & Pesquet, E.
1047 (2015). Proteomic Analysis of Microtubule Interacting Proteins over the Course of Xylem
1048 Tracheary Element Formation in Arabidopsis. *Plant Cell, 27*(10), 2709-2726.
1049 doi:10.1105/tpc.15.00314
1050 Desprez, T., Juraniec, M., Crowell, E. F., Jouy, H., Pochylova, Z., Parcy, F., . . . Vernhettes, S. (2007).
1051 Organization of cellulose synthase complexes involved in primary cell wall synthesis in
1052 Arabidopsis thaliana. *Proc Natl Acad Sci U S A, 104*(39), 15572-15577.
1053 doi:10.1073/pnas.0706569104
1054 Diotallevi, F., & Mulder, B. (2007). The cellulose synthase complex: a polymerization driven
1055 supramolecular motor. *Biophys J, 92*(8), 2666-2673. doi:10.1529/biophysj.106.099473
1056 Drakakaki, G., van de Ven, W., Pan, S., Miao, Y., Wang, J., Keinath, N. F., . . . Raikhel, N. (2012).
1057 Isolation and proteomic analysis of the SYP61 compartment reveal its role in exocytic
1058 trafficking in Arabidopsis. *Cell Res, 22*(2), 413-424. doi:10.1038/cr.2011.129
1059 Durek, P., Schudoma, C., Weckwerth, W., Selbig, J., & Walther, D. (2009). Detection and
1060 characterization of 3D-signature phosphorylation site motifs and their contribution towards
1061 improved phosphorylation site prediction in proteins. *BMC Bioinformatics, 10*, 117.
1062 doi:10.1186/1471-2105-10-117
1063 Endler, A., Kesten, C., Schneider, R., Zhang, Y., Ivakov, A., Froehlich, A., . . . Persson, S. (2015). A
1064 Mechanism for Sustained Cellulose Synthesis during Salt Stress. *Cell, 162*(6), 1353-1364.
1065 doi:10.1016/j.cell.2015.08.028
1066 Engelhardt, J. (1995). Sources, Industrial Derivatives and Commercial Applications of Cellulose.
1067 *Carbohydr. Eur., 12*, 5-14.
1068 Fagard, M., Desnos, T., Desprez, T., Goubet, F., Refregier, G., Mouille, G., . . . Hofte, H. (2000).
1069 PROCUSTE1 encodes a cellulose synthase required for normal cell elongation specifically in
1070 roots and dark-grown hypocotyls of Arabidopsis. *Plant Cell, 12*(12), 2409-2424.
1071 doi:10.1105/tpc.12.12.2409
1072 Felten, J., & Sundberg, B. (2013). Biology, Chemistry and Structure of Tension Wood. . *Cellular*
1073 *Aspects of Wood Formation, Fromm, J. ed: Springer Berlin Heidelberg*, 203-224.
1074 doi:10.1007/978-3-642-36491-4_8,#Springer-Verlag
1075 Fernandes, A. N., Thomas, L. H., Altaner, C. M., Callow, P., Forsyth, V. T., Apperley, D. C., . . . Jarvis,
1076 M. C. (2011). Nanostructure of cellulose microfibrils in spruce wood. *Proc Natl Acad Sci U S*
1077 *A, 108*(47), E1195-1203. doi:10.1073/pnas.1108942108
1078 Fisher, D. D., & Cyr, R. J. (1998). Extending the Microtubule/Microfibril paradigm. Cellulose synthesis
1079 is required for normal cortical microtubule alignment in elongating cells. *Plant Physiol,*
1080 *116*(3), 1043-1051. doi:10.1104/pp.116.3.1043
1081 Foston, M., Hubbell, C. A., Samuel, R., Jung, S., Fan, H., Ding, S., . . . Ragauskas, J. (2011). Chemical,
1082 ultrastructural and supramolecular analysis of tension wood in *Populus tremula* x *alba* as a
1083 model substrate for reduced recalcitrance. *Energy & Environmental Science, 4*, 4962-4971.

1084 Fujita, M., Himmelspach, R., Hocart, C. H., Williamson, R. E., Mansfield, S. D., & Wasteneys, G. O.
1085 (2011). Cortical microtubules optimize cell-wall crystallinity to drive unidirectional growth in
1086 Arabidopsis. *Plant J, 66*(6), 915-928. doi:10.1111/j.1365-313X.2011.04552.x
1087 Fujita, M., Lechner, B., Barton, D. A., Overall, R. L., & Wasteneys, G. O. (2012). The missing link: do
1088 cortical microtubules define plasma membrane nanodomains that modulate cellulose
1089 biosynthesis? *Protoplasma, 249 Suppl 1*, S59-67. doi:10.1007/s00709-011-0332-z
1090 Gadeyne, A., Sanchez-Rodriguez, C., Vanneste, S., Di Rubbo, S., Zauber, H., Vanneste, K., . . . Van
1091 Damme, D. (2014). The TPLATE adaptor complex drives clathrin-mediated endocytosis in
1092 plants. *Cell, 156*(4), 691-704. doi:10.1016/j.cell.2014.01.039
1093 Gardiner, J. C., Taylor, N. G., & Turner, S. R. (2003). Control of cellulose synthase complex localization
1094 in developing xylem. *Plant Cell, 15*(8), 1740-1748. doi:10.1105/tpc.012815
1095 Gardner, K. H., & Blackwell, J. (1974). The structure of native cellulose. *Biopolymers, 13*(10), 1975-
1096 2001. doi:http://dx.doi.org/10.1002/bip.1974.360131005
1097 Giddings, T. H., Jr., Brower, D. L., & Staehelin, L. A. (1980). Visualization of particle complexes in the
1098 plasma membrane of Micrasterias denticulata associated with the formation of cellulose
1099 fibrils in primary and secondary cell walls. *J Cell Biol, 84*(2), 327-339.
1100 doi:10.1083/jcb.84.2.327
1101 Giddings, T. H., Jr., & Staehelin, L. A. (1991). Microtubule-mediated control of microfibril deposition:
1102 A re-examination of the hypothesis. In C. W. Lloyd (Ed.), *In The Cytoskeletal Basis of Plant*
1103 *Growth and Form* (pp. 85-100). San Diego, CA: Academic Press.
1104 Gonneau, M., Desprez, T., Guillot, A., Vernhettes, S., & Hofte, H. (2014). Catalytic subunit
1105 stoichiometry within the cellulose synthase complex. *Plant Physiol, 166*(4), 1709-1712.
1106 doi:10.1104/pp.114.250159
1107 Goss, C. A., Brockmann, D. J., Bushoven, J. T., & Roberts, A. W. (2012). A CELLULOSE SYNTHASE
1108 (CESA) gene essential for gametophore morphogenesis in the moss Physcomitrella patens.
1109 *Planta, 235*(6), 1355-1367. doi:10.1007/s00425-011-1579-5
1110 Green, P. B. (1960). Multinet growth in the cell wall of Nitella. *J Biophys Biochem Cytol, 7*, 289-296.
1111 doi:10.1083/jcb.7.2.289
1112 Green, P. B. (1962). Mechanism for Plant Cellular Morphogenesis. *Science, 138*(3548), 1404-1405.
1113 doi:10.1126/science.138.3548.1404
1114 Gu, Y., Kaplinsky, N., Bringmann, M., Cobb, A., Carroll, A., Sampathkumar, A., . . . Somerville, C. R.
1115 (2010). Identification of a cellulose synthase-associated protein required for cellulose
1116 biosynthesis. *Proc Natl Acad Sci U S A, 107*(29), 12866-12871. doi:10.1073/pnas.1007092107
1117 Guerriero, G., Fugelstad, J., & Bulone, V. (2010). What do we really know about cellulose
1118 biosynthesis in higher plants? *J Integr Plant Biol, 52*(2), 161-175. doi:10.1111/j.1744-
1119 7909.2010.00935.x
1120 Gutierrez, R., Lindeboom, J. J., Paredez, A. R., Emons, A. M., & Ehrhardt, D. W. (2009). Arabidopsis
1121 cortical microtubules position cellulose synthase delivery to the plasma membrane and
1122 interact with cellulose synthase trafficking compartments. *Nat Cell Biol, 11*(7), 797-806.
1123 doi:10.1038/ncb1886
1124 Haigler, C. H., & Brown, R. M. (1986). Transport of rosettes from the golgi apparatus to the plasma
1125 membrane in isolated mesophyll cells ofZinnia elegans during differentiation to tracheary
1126 elements in suspension culture. *Protoplasma, 134*(2-3), 111-120. doi:10.1007/bf01275709
1127 Haigler, C. H., & Roberts, A. W. (2018). Structure/function relationships in the rosette cellulose
1128 synthesis complex illuminated by an evolutionary perspective. *Cellulose, 26*(1), 227-247.
1129 doi:10.1007/s10570-018-2157-9
1130 Hamann, T., Osborne, E., Youngs, H. L., Misson, J., Nussaume, L., & Somerville, C. (2004). Global
1131 expression analysis of CESA and CSL genes in Arabidopsis. *Cellulose, 11*(3/4), 279-286.
1132 doi:10.1023/b:Cell.0000046340.99925.57
1133 Harris, D. M., Corbin, K., Wang, T., Gutierrez, R., Bertolo, A. L., Petti, C., . . . Debolt, S. (2012).
1134 Cellulose microfibril crystallinity is reduced by mutating C-terminal transmembrane region

residues CESA1A903V and CESA3T942I of cellulose synthase. *Proc Natl Acad Sci U S A, 109*(11), 4098-4103. doi:10.1073/pnas.1200352109

Hauser, M. T., Morikami, A., & Benfey, P. N. (1995). Conditional root expansion mutants of *Arabidopsis*. *Development, 121*, 1237-1252.

He, M., Lan, M., Zhang, B., Zhou, Y., Wang, Y., Zhu, L., . . . Fu, Y. (2018). Rab-H1b is essential for trafficking of cellulose synthase and for hypocotyl growth in Arabidopsis thaliana. *J Integr Plant Biol, 60*(11), 1051-1069. doi:10.1111/jipb.12694

Heath, I. B. (1974). A unified hypothesis for the role of membrane bound enzyme complexes and microtubules in plant cell wall synthesis. *J Theor Biol, 48*(2), 445-449. doi:10.1016/s0022-5193(74)80011-1

Hepler, P. K., & Newcomb, E. H. (1964). Microtubules and Fibrils in the Cytoplasm of Coleus Cells Undergoing Secondary Wall Deposition. *J Cell Biol, 20*, 529-532. doi:10.1083/jcb.20.3.529

Hermans, P., de Booys, J., & Maan, C. (1943). Form and mobility of cellulose molecules. *Kolloid-Z, 102*, 169.

Herth, W. (1983). Arrays of plasma-membrane "rosettes" involved in cellulose microfibril formation of Spirogyra. *Planta, 159*(4), 347-356. doi:10.1007/BF00393174

Herth, W. (1985). Plasma-membrane rosettes involved in localized wall thickening during xylem vessel formation of Lepidium sativum L. *Planta, 164*(1), 12-21. doi:10.1007/BF00391020

Hill, J. L., Jr., Hammudi, M. B., & Tien, M. (2014). The Arabidopsis cellulose synthase complex: a proposed hexamer of CESA trimers in an equimolar stoichiometry. *Plant Cell, 26*(12), 4834-4842. doi:10.1105/tpc.114.131193

Hill, J. L., Jr., Hill, A. N., Roberts, A. W., Haigler, C. H., & Tien, M. (2018). Domain swaps of Arabidopsis secondary wall cellulose synthases to elucidate their class specificity. *Plant Direct, 2*(7), e00061. doi:10.1002/pld3.61

Himmelspach, R., Williamson, R. E., & Wasteneys, G. O. (2003). Cellulose microfibril alignment recovers from DCB-induced disruption despite microtubule disorganization. *Plant J, 36*(4), 565-575. doi:10.1046/j.1365-313x.2003.01906.x

Holstein, S. E. (2002). Clathrin and plant endocytosis. *Traffic, 3*(9), 614-620. doi:10.1034/j.1600-0854.2002.30903.x

Jacob-Wilk, D., Kurek, I., Hogan, P., & Delmer, D. P. (2006). The cotton fiber zinc-binding domain of cellulose synthase A1 from Gossypium hirsutum displays rapid turnover in vitro and in vivo. *Proc Natl Acad Sci U S A, 103*(32), 12191-12196. doi:10.1073/pnas.0605098103

Kesten, C., Wallmann, A., Schneider, R., McFarlane, H. E., Diehl, A., Khan, G. A., . . . Persson, S. (2019). The companion of cellulose synthase 1 confers salt tolerance through a Tau-like mechanism in plants. *Nat Commun, 10*(1), 857. doi:10.1038/s41467-019-08780-3

Kim, W. C., Kim, J. Y., Ko, J. H., Kim, J., & Han, K. H. (2013a). Transcription factor MYB46 is an obligate component of the transcriptional regulatory complex for functional expression of secondary wall-associated cellulose synthases in Arabidopsis thaliana. *J Plant Physiol, 170*(15), 1374-1378. doi:10.1016/j.jplph.2013.04.012

Kim, W. C., Ko, J. H., Kim, J. Y., Kim, J., Bae, H. J., & Han, K. H. (2013b). MYB46 directly regulates the gene expression of secondary wall-associated cellulose synthases in Arabidopsis. *Plant Journal, 73*(1), 26-36. doi:10.1111/j.1365-313x.2012.05124

Kimura, S., & Itoh, T. (1996). New cellulose synthesizing complexes (terminal complexes) involved in animal cellulose biosynthesis in the tunicate *Metandrocarpa uedai*. *Protoplasma, 194*(3-4), 151-163. doi:10.1007/bf01882023

Kimura, S., Laosinchai, W., Itoh, T., Cui, X., Linder, C. R., & Brown, R. M., Jr. (1999). Immunogold labeling of rosette terminal cellulose-synthesizing complexes in the vascular plant vigna angularis. . *Plant Cell, 11*(11), 2075-2086. doi:10.1105/tpc.11.11.2075

Ko, J. H., Kim, W. C., & Han, K. H. (2009). Ectopic expression of MYB46 identifies transcriptional regulatory genes involved in secondary wall biosynthesis in Arabidopsis. *Plant J, 60*(4), 649-665. doi:10.1111/j.1365-313X.2009.03989.x

1186 Kumar, M., Atanassov, I., & Turner, S. (2017). Functional Analysis of Cellulose Synthase (CESA)
1187 Protein Class Specificity. *Plant Physiol, 173*(2), 970-983. doi:10.1104/pp.16.01642
1188 Kumar, M., Carr, P., & Turner, S. (2020). doi:10.1101/2020.05.12.090415
1189 Kumar, M., Wightman, R., Atanassov, I., Gupta, A., Hurst, C. H., Hemsley, P. A., & Turner, S. (2016). S-
1190 Acylation of the cellulose synthase complex is essential for its plasma membrane
1191 localization. *Science, 353*(6295), 166-169. doi:10.1126/science.aaf4009
1192 Kurek, I., Kawagoe, Y., Jacob-Wilk, D., Doblin, M., & Delmer, D. (2002). Dimerization of cotton fiber
1193 cellulose synthase catalytic subunits occurs via oxidation of the zinc-binding domains. *Proc*
1194 *Natl Acad Sci U S A, 99*(17), 11109-11114. doi:10.1073/pnas.162077099
1195 Lai-Kee-Him, J., Chanzy, H., Muller, M., Putaux, J. L., Imai, T., & Bulone, V. (2002). In vitro versus in
1196 vivo cellulose microfibrils from plant primary wall synthases: structural differences. *J Biol*
1197 *Chem, 277*(40), 36931-36939. doi:10.1074/jbc.M203530200
1198 Lampugnani, E. R., Flores-Sandoval, E., Tan, Q. W., Mutwil, M., Bowman, J. L., & Persson, S. (2019).
1199 Cellulose Synthesis - Central Components and Their Evolutionary Relationships. *Trends Plant*
1200 *Sci, 24*(5), 402-412. doi:10.1016/j.tplants.2019.02.011
1201 Ledbetter, M. C., & Porter, K. R. (1963). A "Microtubule" in Plant Cell Fine Structure. *J Cell Biol, 19*(1),
1202 239-250. doi:10.1083/jcb.19.1.239
1203 Lei, L., Singh, A., Bashline, L., Li, S., Yingling, Y. G., & Gu, Y. (2015). CELLULOSE SYNTHASE
1204 INTERACTIVE1 Is Required for Fast Recycling of Cellulose Synthase Complexes to the Plasma
1205 Membrane in Arabidopsis. *Plant Cell, 27*(10), 2926-2940. doi:10.1105/tpc.15.00442
1206 Lei, L., Zhang, T., Strasser, R., Lee, C. M., Gonneau, M., Mach, L., . . . Gu, Y. (2014). The jiaoyao1
1207 Mutant Is an Allele of korrigan1 That Abolishes Endoglucanase Activity and Affects the
1208 Organization of Both Cellulose Microfibrils and Microtubules in Arabidopsis. *Plant Cell, 26*(6),
1209 2601-2616. doi:10.1105/tpc.114.126193
1210 Li, S., Bashline, L., Lei, L., & Gu, Y. (2014). Cellulose synthesis and its regulation. *Arabidopsis Book, 12*,
1211 e0169. doi:10.1199/tab.0169
1212 Li, S., Bashline, L., Zheng, Y., Xin, X., Huang, S., Kong, Z., . . . Gu, Y. (2016). Cellulose synthase
1213 complexes act in a concerted fashion to synthesize highly aggregated cellulose in secondary
1214 cell walls of plants. *Proc Natl Acad Sci U S A, 113*(40), 11348-11353.
1215 doi:10.1073/pnas.1613273113
1216 Li, S., Lei, L., & Gu, Y. (2013). Functional analysis of complexes with mixed primary and secondary
1217 cellulose synthases. *Plant Signal Behav, 8*(3), e23179. doi:10.4161/psb.23179
1218 Li, S., Lei, L., Somerville, C. R., & Gu, Y. (2012). Cellulose synthase interactive protein 1 (CSI1) links
1219 microtubules and cellulose synthase complexes. *Proc Natl Acad Sci U S A, 109*(1), 185-190.
1220 doi:10.1073/pnas.1118560109
1221 Li, S., Lei, L., Yingling, Y. G., & Gu, Y. (2015). Microtubules and cellulose biosynthesis: the emergence
1222 of new players. *Curr Opin Plant Biol, 28*, 76-82. doi:10.1016/j.pbi.2015.09.002
1223 Li, X., Speicher, T. L., Dees, D., Mansoori, N., McManus, J. B., Tien, M., . . . Roberts, A. W. (2019).
1224 Convergent evolution of hetero-oligomeric cellulose synthesis complexes in mosses and
1225 seed plants. *Plant J, 99*(5), 862-876. doi:10.1111/tpj.14366
1226 Liu, L., Shang-Guan, K., Zhang, B., Liu, X., Yan, M., Zhang, L., . . . Zhou, Y. (2013). Brittle Culm1, a
1227 COBRA-like protein, functions in cellulose assembly through binding cellulose microfibrils.
1228 *PLoS Genet, 9*(8), e1003704. doi:10.1371/journal.pgen.1003704
1229 Liu, Z., Schneider, R., Kesten, C., Zhang, Y., Somssich, M., Zhang, Y., . . . Persson, S. (2016). Cellulose-
1230 Microtubule Uncoupling Proteins Prevent Lateral Displacement of Microtubules during
1231 Cellulose Synthesis in Arabidopsis. *Dev Cell, 38*(3), 305-315.
1232 doi:10.1016/j.devcel.2016.06.032
1233 Luo, Y., Scholl, S., Doering, A., Zhang, Y., Irani, N. G., Rubbo, S. D., . . . Russinova, E. (2015). V-ATPase
1234 activity in the TGN/EE is required for exocytosis and recycling in Arabidopsis. *Nat Plants, 1*,
1235 15094. doi:10.1038/nplants.2015.94

MacMillan, C. P., Birke, H., Chuah, A., Brill, E., Tsuji, Y., Ralph, J., . . . Pettolino, F. A. (2017). Tissue and cell-specific transcriptomes in cotton reveal the subtleties of gene regulation underlying the diversity of plant secondary cell walls. *BMC Genomics, 18*(1), 539. doi:10.1186/s12864-017-3902-4

Maloney, V. J., & Mansfield, S. D. (2010). Characterization and varied expression of a membrane-bound endo-beta-1,4-glucanase in hybrid poplar. *Plant Biotechnol J, 8*(3), 294-307. doi:10.1111/j.1467-7652.2009.00483.x

Mansoori, N., Timmers, J., Desprez, T., Alvim-Kamei, C. L., Dees, D. C., Vincken, J. P., . . . Trindade, L. M. (2014). KORRIGAN1 interacts specifically with integral components of the cellulose synthase machinery. *PLoS One, 9*(11), e112387. doi:10.1371/journal.pone.0112387

Marga, F., Grandbois, M., Cosgrove, D. J., & Baskin, T. I. (2005). Cell wall extension results in the coordinate separation of parallel microfibrils: evidence from scanning electron microscopy and atomic force microscopy. *Plant J, 43*(2), 181-190. doi:10.1111/j.1365-313X.2005.02447.x

Martinez-Sanz, M., Pettolino, F., Flanagan, B., Gidley, M. J., & Gilbert, E. P. (2017). Structure of cellulose microfibrils in mature cotton fibres. *Carbohydr Polym, 175*, 450-463. doi:10.1016/j.carbpol.2017.07.090

McCarthy, R. L., Zhong, R. Q., & Ye, Z. H. (2009). MYB83 Is a Direct Target of SND1 and Acts Redundantly with MYB46 in the Regulation of Secondary Cell Wall Biosynthesis in Arabidopsis. *Plant and Cell Physiology, 50*(11), 1950-1964. doi:10.1093/pcp/pcp139

McFarlane, H. E., Doring, A., & Persson, S. (2014). The cell biology of cellulose synthesis. *Annu Rev Plant Biol, 65*, 69-94. doi:10.1146/annurev-arplant-050213-040240

Meents, M. J., Watanabe, Y., & Samuels, A. L. (2018). The cell biology of secondary cell wall biosynthesis. *Ann Bot, 121*(6), 1107-1125. doi:10.1093/aob/mcy005

Mendu, V., Griffiths, J. S., Persson, S., Stork, J., Downie, A. B., Voiniciuc, C., . . . DeBolt, S. (2011). Subfunctionalization of cellulose synthases in seed coat epidermal cells mediates secondary radial wall synthesis and mucilage attachment. *Plant Physiol, 157*(1), 441-453. doi:10.1104/pp.111.179069

Mizuta, S., & Brown, R. M. (1992). High resolution analysis of the formation of cellulose synthesizing complexes inVaucheria hamata. *Protoplasma, 166*(3-4), 187-199. doi:10.1007/bf01322781

Mizuta, S., & Okuda, K. (1987). Boodlea Cell Wall Microfibril Orientation Unrelated to Cortical Microtubule Arrangement *Botanical Gazette, 148*(3), 297-307.

Morejohn, L. (1991). The molecular pharmacology of plant tubulin and microtubules. In C. W. Lloyd (Ed.), *The Cytoskeletal Basis of Plant Growth and Form* (pp. 29-44). San Diego, CA: Academic Press.

Morgan, J. L., McNamara, J. T., Fischer, M., Rich, J., Chen, H. M., Withers, S. G., & Zimmer, J. (2016). Observing cellulose biosynthesis and membrane translocation in crystallo. *Nature, 531*(7594), 329-334. doi:10.1038/nature16966

Morgan, J. L., Strumillo, J., & Zimmer, J. (2013). Crystallographic snapshot of cellulose synthesis and membrane translocation. *Nature, 493*(7431), 181-186. doi:10.1038/nature11744

Mueller, S. C., & Brown, R. M., Jr. (1980). Evidence for an intramembrane component associated with a cellulose microfibril-synthesizing complex in higher plants. *J Cell Biol, 84*(2), 315-326. doi:10.1083/jcb.84.2.315

Müller, M., Burghammer, M., & Sugiyama, J. (2006). Direct investigation of the structural properties of tension wood cellulose microfibrils using microbeam X-ray fibre diffraction. *Holzforschung, 60*(5), 474-479. doi:10.1515/hf.2006.078

Neumann, U., Brandizzi, F., & Hawes, C. (2003). Protein transport in plant cells: in and out of the Golgi. *Ann Bot, 92*(2), 167-180. doi:10.1093/aob/mcg134

Newman, R., & Hemmingson, J. (1990). Determination of the Degree of Cellulose Crystallinity in Wood by Carbon-13 Nuclear Magnetic Resonance Spectroscopy. *Holzforschung, 44*(5), 351-355.

1286 Newman, R. H., Hill, S. J., & Harris, P. J. (2013). Wide-angle x-ray scattering and solid-state nuclear
1287 magnetic resonance data combined to test models for cellulose microfibrils in mung bean
1288 cell walls. *Plant Physiol, 163*(4), 1558-1567. doi:10.1104/pp.113.228262
1289 Nicol, F., His, I., Jauneau, A., Vernhettes, S., Canut, H., & Hofte, H. (1998). A plasma membrane-
1290 bound putative endo-1,4-beta-D-glucanase is required for normal wall assembly and cell
1291 elongation in Arabidopsis. *EMBO J, 17*(19), 5563-5576. doi:10.1093/emboj/17.19.5563
1292 Niimura, H., Yokoyama, T., Kimura, S., Matsumoto, Y., & Kuga, S. (2009). AFM observation of
1293 ultrathin microfibrils in fruit tissues. *Cellulose, 17*(1), 13-18. doi:10.1007/s10570-009-9361-6
1294 Nixon, B. T., Mansouri, K., Singh, A., Du, J., Davis, J. K., Lee, J. G., . . . Haigler, C. H. (2016).
1295 Comparative Structural and Computational Analysis Supports Eighteen Cellulose Synthases
1296 in the Plant Cellulose Synthesis Complex. *Sci Rep, 6*, 28696. doi:10.1038/srep28696
1297 Norris, J. H., Li, X., Huang, S., Van de Meene, A. M. L., Tran, M. L., Killeavy, E., . . . Roberts, A. W.
1298 (2017). Functional Specialization of Cellulose Synthase Isoforms in a Moss Shows Parallels
1299 with Seed Plants. *Plant Physiol, 175*(1), 210-222. doi:10.1104/pp.17.00885
1300 Nuhse, T. S., Stensballe, A., Jensen, O. N., & Peck, S. C. (2004). Phosphoproteomics of the Arabidopsis
1301 plasma membrane and a new phosphorylation site database. *Plant Cell, 16*(9), 2394-2405.
1302 doi:10.1105/tpc.104.023150
1303 Ohlsson, A. B., Djerbi, S., Winzell, A., Bessueille, L., Staldal, V., Li, X., . . . Berglund, T. (2006). Cell
1304 suspension cultures of Populus tremula x P. tremuloides exhibit a high level of cellulose
1305 synthase gene expression that coincides with increased in vitro cellulose synthase activity.
1306 *Protoplasma, 228*(4), 221-229. doi:10.1007/s00709-006-0156-4
1307 Olek, A. T., Rayon, C., Makowski, L., Kim, H. R., Ciesielski, P., Badger, J., . . . Carpita, N. C. (2014). The
1308 structure of the catalytic domain of a plant cellulose synthase and its assembly into dimers.
1309 *Plant Cell, 26*(7), 2996-3009. doi:10.1105/tpc.114.126862
1310 Pagant, S., Bichet, A., Sugimoto, K., Lerouxel, O., Desprez, T., McCann, M., . . . Hofte, H. (2002).
1311 KOBITO1 encodes a novel plasma membrane protein necessary for normal synthesis of
1312 cellulose during cell expansion in Arabidopsis. *Plant Cell, 14*(9), 2001-2013.
1313 doi:10.1105/tpc.002873
1314 Paredez, A. R., Persson, S., Ehrhardt, D. W., & Somerville, C. R. (2008). Genetic evidence that
1315 cellulose synthase activity influences microtubule cortical array organization. *Plant Physiol,*
1316 *147*(4), 1723-1734. doi:10.1104/pp.108.120196
1317 Paredez, A. R., Somerville, C. R., & Ehrhardt, D. W. (2006). Visualization of cellulose synthase
1318 demonstrates functional association with microtubules. *Science, 312*(5779), 1491-1495.
1319 doi:10.1126/science.1126551
1320 Park, S., Song, B., Shen, W., & Ding, S. Y. (2019). A mutation in the catalytic domain of cellulose
1321 synthase 6 halts its transport to the Golgi apparatus. *J Exp Bot, 70*(21), 6071-6083.
1322 doi:10.1093/jxb/erz369
1323 Pear, J. R., Kawagoe, Y., Schreckengost, W. E., Delmer, D. P., & Stalker, D. M. (1996). Higher plants
1324 contain homologs of the bacterial celA genes encoding the catalytic subunit of cellulose
1325 synthase. *Proc Natl Acad Sci U S A, 93*(22), 12637-12642. doi:10.1073/pnas.93.22.12637
1326 Persson, S., Paredez, A., Carroll, A., Palsdottir, H., Doblin, M., Poindexter, P., . . . Somerville, C. R.
1327 (2007). Genetic evidence for three unique components in primary cell-wall cellulose
1328 synthase complexes in Arabidopsis. *Proc Natl Acad Sci U S A, 104*(39), 15566-15571.
1329 doi:10.1073/pnas.0706592104
1330 Polko, J. K., Barnes, W. J., Voiniciuc, C., Doctor, S., Steinwand, B., Hill, J. L., Jr., . . . Kieber, J. J. (2018).
1331 SHOU4 Proteins Regulate Trafficking of Cellulose Synthase Complexes to the Plasma
1332 Membrane. *Curr Biol, 28*(19), 3174-3182 e3176. doi:10.1016/j.cub.2018.07.076
1333 Preston, R. D. (1974). *The Physical Biology of Plant Cell Walls*.
1334 Preston, R. D., Nicolai, E. R., & Millard, A. (1948). An electron microscope study of cellulose in the
1335 wall of *Valonia ventricosa*. *Nature, 162*(4121), 665-667. doi:10.1038/162665a0.

1336 Purushotham, P., Cho, S. H., Diaz-Moreno, S. M., Kumar, M., Nixon, B. T., Bulone, V., & Zimmer, J.
1337 (2016). A single heterologously expressed plant cellulose synthase isoform is sufficient for
1338 cellulose microfibril formation in vitro. *Proc Natl Acad Sci U S A, 113*(40), 11360-11365.
1339 doi:10.1073/pnas.1606210113
1340 Purushotham, P., Ho, R., & Zimmer, J. (2020). Architecture of a catalytically active homotrimeric
1341 plant cellulose synthase complex. *Science*. doi:10.1126/science.abb2978
1342 Rao, X., & Dixon, R. A. (2018). Current Models for Transcriptional Regulation of Secondary Cell Wall
1343 Biosynthesis in Grasses. *Front Plant Sci, 9*, 399. doi:10.3389/fpls.2018.00399
1344 Refregier, G., Pelletier, S., Jaillard, D., & Hofte, H. (2004). Interaction between wall deposition and
1345 cell elongation in dark-grown hypocotyl cells in Arabidopsis. *Plant Physiol, 135*(2), 959-968.
1346 doi:10.1104/pp.104.038711
1347 Reynolds, G. D., Wang, C., Pan, J., & Bednarek, S. Y. (2018). Inroads into Internalization: Five Years of
1348 Endocytic Exploration. *Plant Physiol, 176*(1), 208-218. doi:10.1104/pp.17.01117
1349 Richmond, T. (2000). Higher plant cellulose synthases. *Genome Biol, 1*(4), REVIEWS3001.
1350 doi:10.1186/gb-2000-1-4-reviews3001
1351 Roberts, A. W., & Bushoven, J. T. (2007). The cellulose synthase (CESA) gene superfamily of the moss
1352 Physcomitrella patens. *Plant Mol Biol, 63*(2), 207-219. doi:10.1007/s11103-006-9083-1
1353 Roelofsen, P. A. (1958). Cell-Wall Structure as Related to Surface Growth Some Supplementary
1354 Remarks on Multinet Growth. *Acta Botanica Neerlandica, 7*(1), 77-89. doi:10.1111/j.1438-
1355 8677.1958.tb00609.x
1356 Roelofsen, P. A., & Houwink, A. L. (1951). Cell wall structure of staminal hairs ofTradescantia virginica
1357 and its relation with growth. *Protoplasma, 40*(1), 1-22. doi:10.1007/bf01247932
1358 Roelofsen, P. A., & Houwink, A. L. (1953). Architecture and Growth of the Primary Cell Wall in Some
1359 Plant Hairs and in the Phycomyces Sporangiophore. *Acta Botanica Neerlandica, 2*(2), 218-
1360 225. doi:10.1111/j.1438-8677.1953.tb00272.x
1361 Roudier, F., Fernandez, A. G., Fujita, M., Himmelspach, R., Borner, G. H., Schindelman, G., . . . Benfey,
1362 P. N. (2005). COBRA, an Arabidopsis extracellular glycosyl-phosphatidyl inositol-anchored
1363 protein, specifically controls highly anisotropic expansion through its involvement in
1364 cellulose microfibril orientation. *Plant Cell, 17*(6), 1749-1763. doi:10.1105/tpc.105.031732
1365 Rushton, P. S., Olek, A. T., Makowski, L., Badger, J., Steussy, C. N., Carpita, N. C., & Stauffacher, C. V.
1366 (2017). Rice Cellulose SynthaseA8 Plant-Conserved Region Is a Coiled-Coil at the Catalytic
1367 Core Entrance. *Plant Physiol, 173*(1), 482-494. doi:10.1104/pp.16.00739
1368 Saelim, L., Akiyoshi, N., Tan, T. T., Ihara, A., Yamaguchi, M., Hirano, K., . . . Ohtani, M. (2019).
1369 Arabidopsis Group IIId ERF proteins positively regulate primary cell wall-type CESA genes. *J*
1370 *Plant Res, 132*(1), 117-129. doi:10.1007/s10265-018-1074-1
1371 Sakamoto, S., Somssich, M., Nakata, M. T., Unda, F., Atsuzawa, K., Kaneko, Y., . . . Mitsuda, N. (2018).
1372 Complete substitution of a secondary cell wall with a primary cell wall in Arabidopsis. *Nat*
1373 *Plants, 4*(10), 777-783. doi:10.1038/s41477-018-0260-4
1374 Sampathkumar, A., Gutierrez, R., McFarlane, H. E., Bringmann, M., Lindeboom, J., Emons, A. M., . . .
1375 Persson, S. (2013). Patterning and lifetime of plasma membrane-localized cellulose synthase
1376 is dependent on actin organization in Arabidopsis interphase cells. *Plant Physiol, 162*(2), 675-
1377 688. doi:10.1104/pp.113.215277
1378 Sanchez-Rodriguez, C., Ketelaar, K., Schneider, R., Villalobos, J. A., Somerville, C. R., Persson, S., &
1379 Wallace, I. S. (2017). BRASSINOSTEROID INSENSITIVE2 negatively regulates cellulose
1380 synthesis in Arabidopsis by phosphorylating cellulose synthase 1. *Proc Natl Acad Sci U S A,*
1381 *114*(13), 3533-3538. doi:10.1073/pnas.1615005114
1382 Sanchez-Rodriguez, C., Shi, Y., Kesten, C., Zhang, D., Sancho-Andres, G., Ivakov, A., . . . Persson, S.
1383 (2018). The Cellulose Synthases Are Cargo of the TPLATE Adaptor Complex. *Mol Plant, 11*(2),
1384 346-349. doi:10.1016/j.molp.2017.11.012
1385 Saxena, I. M., & Brown, R. M., Jr. (2005). Cellulose biosynthesis: current views and evolving concepts.
1386 *Ann Bot, 96*(1), 9-21. doi:10.1093/aob/mci155

1387 Saxena, I. M., Brown, R. M., Jr., & Dandekar, T. (2001). Structure--function characterization of
1388 cellulose synthase: relationship to other glycosyltransferases. *Phytochemistry, 57*(7), 1135-
1389 1148. doi:10.1016/s0031-9422(01)00048-6
1390 Saxena, I. M., Lin, F. C., & Brown, R. M., Jr. (1990). Cloning and sequencing of the cellulose synthase
1391 catalytic subunit gene of Acetobacter xylinum. *Plant Mol Biol, 15*(5), 673-683.
1392 doi:10.1007/bf00016118
1393 Scavuzzo-Duggan, T. R., Chaves, A. M., Singh, A., Sethaphong, L., Slabaugh, E., Yingling, Y. G., . . .
1394 Roberts, A. W. (2018). Cellulose synthase 'class specific regions' are intrinsically disordered
1395 and functionally undifferentiated. *J Integr Plant Biol, 60*(6), 481-497. doi:10.1111/jipb.12637
1396 Schneider, R., Tang, L., Lampugnani, E. R., Barkwill, S., Lathe, R., Zhang, Y., . . . Persson, S. (2017). Two
1397 Complementary Mechanisms Underpin Cell Wall Patterning during Xylem Vessel
1398 Development. *Plant Cell, 29*(10), 2433-2449. doi:10.1105/tpc.17.00309
1399 Sethaphong, L., Davis, J. K., Slabaugh, E., Singh, A., Haigler, C. H., & Yingling, Y. G. (2016). Prediction
1400 of the structures of the plant-specific regions of vascular plant cellulose synthases and
1401 correlated functional analysis. *Cellulose, 23*(1), 145-161. doi:10.1007/s10570-015-0789-6
1402 Sethaphong, L., Haigler, C. H., Kubicki, J. D., Zimmer, J., Bonetta, D., DeBolt, S., & Yingling, Y. G.
1403 (2013). Tertiary model of a plant cellulose synthase. *Proc Natl Acad Sci U S A, 110*(18), 7512-
1404 7517. doi:10.1073/pnas.1301027110
1405 Slabaugh, E., Scavuzzo-Duggan, T., Chaves, A., Wilson, L., Wilson, C., Davis, J. K., . . . Haigler, C. H.
1406 (2016). The valine and lysine residues in the conserved FxVTxK motif are important for the
1407 function of phylogenetically distant plant cellulose synthases. *Glycobiology, 26*(5), 509-519.
1408 doi:10.1093/glycob/cwv118
1409 Somerville, C. (2006). Cellulose synthesis in higher plants. *Annu Rev Cell Dev Biol, 22*, 53-78.
1410 doi:10.1146/annurev.cellbio.22.022206.160206
1411 Song, B., Zhao, S., Shen, W., Collings, C., & Ding, S. Y. (2020). Direct Measurement of Plant Cellulose
1412 Microfibril and Bundles in Native Cell Walls. *Front Plant Sci, 11*, 479.
1413 doi:10.3389/fpls.2020.00479
1414 Song, D., Shen, J., & Li, L. (2010). Characterization of cellulose synthase complexes in Populus xylem
1415 differentiation. *New Phytol, 187*(3), 777-790. doi:10.1111/j.1469-8137.2010.03315.x
1416 Speicher, T. L., Li, P. Z., & Wallace, I. S. (2018). Phosphoregulation of the Plant Cellulose Synthase
1417 Complex and Cellulose Synthase-Like Proteins. *Plants (Basel), 7*(3).
1418 doi:10.3390/plants7030052
1419 Strabala, T. J., & Macmillan, C. P. (2013). The Arabidopsis wood model-the case for the inflorescence
1420 stem. *Plant Sci, 210*, 193-205. doi:10.1016/j.plantsci.2013.05.007
1421 Strasser, R. (2018). Protein Quality Control in the Endoplasmic Reticulum of Plants. *Annu Rev Plant*
1422 *Biol, 69*, 147-172. doi:10.1146/annurev-arplant-042817-040331
1423 Sugimoto, K., Himmelspach, R., Williamson, R. E., & Wasteneys, G. O. (2003). Mutation or drug-
1424 dependent microtubule disruption causes radial swelling without altering parallel cellulose
1425 microfibril deposition in Arabidopsis root cells. *Plant Cell, 15*(6), 1414-1429.
1426 doi:10.1105/tpc.011593
1427 Suslov, D., Verbelen, J. P., & Vissenberg, K. (2009). Onion epidermis as a new model to study the
1428 control of growth anisotropy in higher plants. *J Exp Bot, 60*(14), 4175-4187.
1429 doi:10.1093/jxb/erp251
1430 Szyjanowicz, P. M., McKinnon, I., Taylor, N. G., Gardiner, J., Jarvis, M. C., & Turner, S. R. (2004). The
1431 irregular xylem 2 mutant is an allele of korrigan that affects the secondary cell wall of
1432 Arabidopsis thaliana. *Plant J, 37*(5), 730-740. doi:10.1111/j.1365-313x.2003.02000.x
1433 Taylor, N. G. (2007). Identification of cellulose synthase AtCesA7 (IRX3) in vivo phosphorylation sites-
1434 -a potential role in regulating protein degradation. *Plant Mol Biol, 64*(1-2), 161-171.
1435 doi:10.1007/s11103-007-9142-2

1436 Taylor, N. G., Howells, R. M., Huttly, A. K., Vickers, K., & Turner, S. R. (2003). Interactions among
1437 three distinct CesA proteins essential for cellulose synthesis. *Proc Natl Acad Sci U S A, 100*(3),
1438 1450-1455. doi:10.1073/pnas.0337628100
1439 Thomas, L. H., Forsyth, V. T., Sturcova, A., Kennedy, C. J., May, R. P., Altaner, C. M., . . . Jarvis, M. C.
1440 (2013). Structure of cellulose microfibrils in primary cell walls from collenchyma. *Plant*
1441 *Physiol, 161*(1), 465-476. doi:10.1104/pp.112.206359
1442 Tsekos, I. (1999). The Sites of Cellulose Synthesis in Algae: Diversity and Evolution of Cellulose-
1443 Synthesizing Enzyme Complexes. *Journal of Phycology, 35*(4), 635-655. doi:10.1046/j.1529-
1444 8817.1999.3540635.x
1445 Turner, S. R., & Somerville, C. R. (1997). Collapsed xylem phenotype of Arabidopsis identifies
1446 mutants deficient in cellulose deposition in the secondary cell wall. *Plant Cell, 9*(5), 689-701.
1447 doi:10.1105/tpc.9.5.689
1448 Uemura, T., Kim, H., Saito, C., Ebine, K., Ueda, T., Schulze-Lefert, P., & Nakano, A. (2012). Qa-SNAREs
1449 localized to the trans-Golgi network regulate multiple transport pathways and extracellular
1450 disease resistance in plants. *Proc Natl Acad Sci U S A, 109*(5), 1784-1789.
1451 doi:10.1073/pnas.1115146109
1452 Vain, T., Crowell, E. F., Timpano, H., Biot, E., Desprez, T., Mansoori, N., . . . Vernhettes, S. (2014). The
1453 Cellulase KORRIGAN Is Part of the Cellulose Synthase Complex. *Plant Physiol, 165*(4), 1521-
1454 1532. doi:10.1104/pp.114.241216
1455 Vandavasi, V. G., Putnam, D. K., Zhang, Q., Petridis, L., Heller, W. T., Nixon, B. T., . . . O'Neill, H.
1456 (2016). A Structural Study of CESA1 Catalytic Domain of Arabidopsis Cellulose Synthesis
1457 Complex: Evidence for CESA Trimers. *Plant Physiol, 170*(1), 123-135.
1458 doi:10.1104/pp.15.01356
1459 Vergara, C. E., & Carpita, N. C. (2001). Beta-D-glycan Synthases and the CesA Gene Family: Lessons to
1460 Be Learned From the Mixed-Linkage (1-->3),(1-->4)beta-D-glucan Synthase *Plant Mol Biol,*
1461 *47*, 145-160.
1462 Vernoud, V., Horton, A. C., Yang, Z., & Nielsen, E. (2003). Analysis of the small GTPase gene
1463 superfamily of Arabidopsis. *Plant Physiol, 131*(3), 1191-1208. doi:10.1104/pp.013052
1464 Viotti, C., Bubeck, J., Stierhof, Y. D., Krebs, M., Langhans, M., van den Berg, W., . . . Schumacher, K.
1465 (2010). Endocytic and secretory traffic in Arabidopsis merge in the trans-Golgi network/early
1466 endosome, an independent and highly dynamic organelle. *Plant Cell, 22*(4), 1344-1357.
1467 doi:10.1105/tpc.109.072637
1468 Wang, J., Howles, P. A., Cork, A. H., Birch, R. J., & Williamson, R. E. (2006). Chimeric proteins suggest
1469 that the catalytic and/or C-terminal domains give CesA1 and CesA3 access to their specific
1470 sites in the cellulose synthase of primary walls. *Plant Physiol, 142*(2), 685-695.
1471 doi:10.1104/pp.106.084004
1472 Watanabe, Y., Meents, M. J., McDonnell, L. M., Barkwill, S., Sampathkumar, A., Cartwright, H. N., . . .
1473 Mansfield, S. D. (2015). Visualization of cellulose synthases in Arabidopsis secondary cell
1474 walls. *Science, 350*(6257), 198-203. doi:10.1126/science.aac7446
1475 Watanabe, Y., Schneider, R., Barkwill, S., Gonzales-Vigil, E., Hill, J. L., Jr., Samuels, A. L., . . . Mansfield,
1476 S. D. (2018). Cellulose synthase complexes display distinct dynamic behaviors during xylem
1477 transdifferentiation. *Proc Natl Acad Sci U S A, 115*(27), E6366-E6374.
1478 doi:10.1073/pnas.1802113115
1479 Wiedemeier, A. M. D., Judy-March, J. E., Hocart, C. H., Wasteneys, G. O., Williamson, R. E., & Baskin,
1480 T. I. (2002). Mutant alleles of *Arabidopsis RADIALLY SWOLLEN 4* and *7* reduce growth
1481 anisotropy without altering the transverse orientation of cortical microtubules or cellulose
1482 microfibrils. *Development, 129*, 4821-4830.
1483 Wightman, R., & Turner, S. R. (2008). The roles of the cytoskeleton during cellulose deposition at the
1484 secondary cell wall. *Plant J, 54*(5), 794-805. doi:10.1111/j.1365-313X.2008.03444.x
1485 Wolf, S., Hematy, K., & Hofte, H. (2012). Growth control and cell wall signaling in plants. *Annu Rev*
1486 *Plant Biol, 63*, 381-407. doi:10.1146/annurev-arplant-042811-105449

1487 Wong, H. C., Fear, A. L., Calhoon, R. D., Eichinger, G. H., Mayer, R., Amikam, D., . . . et al. (1990).
1488 Genetic organization of the cellulose synthase operon in Acetobacter xylinum. *Proc Natl*
1489 *Acad Sci U S A, 87*(20), 8130-8134. doi:10.1073/pnas.87.20.8130
1490 Xie, L., Yang, C., & Wang, X. (2011). Brassinosteroids can regulate cellulose biosynthesis by
1491 controlling the expression of CESA genes in Arabidopsis. *J Exp Bot, 62*(13), 4495-4506.
1492 doi:10.1093/jxb/err164
1493 Xin, X., Lei, L., Zheng, Y., Zhang, T., Pingali, S. V., O'Neill, H., . . . Gu, Y. (2020). CELLULOSE SYNTHASE
1494 INTERACTIVE1 and Microtubule-Dependent Cell Wall Architecture Is Required for Acid
1495 Growth in Arabidopsis Hypocotyls. *J Exp Bot*. doi:10.1093/jxb/eraa063
1496 Yamaguchi, M., Goue, N., Igarashi, H., Ohtani, M., Nakano, Y., Mortimer, J. C., . . . Demura, T. (2010).
1497 VASCULAR-RELATED NAC-DOMAIN6 and VASCULAR-RELATED NAC-DOMAIN7 effectively
1498 induce transdifferentiation into xylem vessel elements under control of an induction system.
1499 *Plant Physiol, 153*(3), 906-914. doi:10.1104/pp.110.154013
1500 Zhang, J., Xie, M., Tuskan, G. A., Muchero, W., & Chen, J. G. (2018a). Recent Advances in the
1501 Transcriptional Regulation of Secondary Cell Wall Biosynthesis in the Woody Plants. *Front*
1502 *Plant Sci, 9*, 1535. doi:10.3389/fpls.2018.01535
1503 Zhang, T., Zheng, Y., & Cosgrove, D. J. (2016a). Spatial organization of cellulose microfibrils and
1504 matrix polysaccharides in primary plant cell walls as imaged by multichannel atomic force
1505 microscopy. *Plant J, 85*(2), 179-192. doi:10.1111/tpj.13102
1506 Zhang, W., Cai, C., & Staiger, C. J. (2019). Myosins XI Are Involved in Exocytosis of Cellulose Synthase
1507 Complexes. *Plant Physiol, 179*(4), 1537-1555. doi:10.1104/pp.19.00018
1508 Zhang, X., Dominguez, P. G., Kumar, M., Bygdell, J., Miroshnichenko, S., Sundberg, B., . . . Niittyla.
1509 (2018b). Cellulose Synthase Stoichiometry in Aspen Differs from Arabidopsis and Norway
1510 Spruce. *Plant Physiol, 177*(3), 1096-1107. doi:10.1104/pp.18.00394
1511 Zhang, Y., Nikolovski, N., Sorieul, M., Vellosillo, T., McFarlane, H. E., Dupree, R., . . . Dupree, P.
1512 (2016b). Golgi-localized STELLO proteins regulate the assembly and trafficking of cellulose
1513 synthase complexes in Arabidopsis. *Nat Commun, 7*, 11656. doi:10.1038/ncomms11656
1514 Zhong, R., Lee, C., Zhou, J., McCarthy, R. L., & Ye, Z. H. (2008). A battery of transcription factors
1515 involved in the regulation of secondary cell wall biosynthesis in Arabidopsis. *Plant Cell,*
1516 *20*(10), 2763-2782. doi:10.1105/tpc.108.061325
1517 Zhong, R., Richardson, E. A., & Ye, Z. H. (2007). Two NAC domain transcription factors, SND1 and
1518 NST1, function redundantly in regulation of secondary wall synthesis in fibers of Arabidopsis.
1519 *Planta, 225*(6), 1603-1611. doi:10.1007/s00425-007-0498-y
1520 Zhu, X., Li, S., Pan, S., Xin, X., & Gu, Y. (2018). CSI1, PATROL1, and exocyst complex cooperate in
1521 delivery of cellulose synthase complexes to the plasma membrane. *Proc Natl Acad Sci U S A,*
1522 *115*(15), E3578-E3587. doi:10.1073/pnas.1800182115
1523 Zhu, X., Xin, X., & Gu, Y. (2019). Cellulose and Hemicellulose Synthesis and Their Regulation in Plant
1524 Cells. In E. Cohen & H. Merzendorfer (Eds.), *Extracellular Sugar-Based Biopolymers Matrices.*
1525 *Biologically-Inspired System* (Vol. 12): Springer, Cham.

1526